

## ORIGINAL RESEARCH ARTICLE

# Endothelial Transcription Factor EB Protects Against Doxorubicin-Induced Endothelial Toxicity and Cardiac Dysfunction

Wa Du<sup>ID</sup>, MD, PhD; Madison Ringer<sup>ID</sup>; Wei Huang<sup>ID</sup>; Darshini Desai, Golam Iftakhar Khandakar; Luis Tron Esqueda<sup>ID</sup>; Chenran Wang; Jun-Lin Guan; Richard C. Becker<sup>ID</sup>; Sakthivel Sadayappan<sup>ID</sup>; Guo-Chang Fan<sup>ID</sup>; Yigang Wang<sup>ID</sup>; Yanbo Fan<sup>ID</sup>, MD, PhD

**BACKGROUND:** Doxorubicin (DOX), an effective chemotherapeutic drug for various cancers, has been demonstrated to induce cardiovascular toxicity in cancer survivors. Endothelial cell (EC) dysfunction is recognized to play a critical role in the onset and severity of cardiotoxicity associated with DOX. TFEB (transcription factor EB), a master regulator of autophagy and lysosome biogenesis, regulates cardiovascular homeostasis. In the present study, we aimed to test whether endothelial TFEB protects against EC damage and alleviates cardiac dysfunction induced by DOX treatment.

**METHODS:** EC-specific TFEB transgenic mice, EC-specific TFEB knockout mice, and their corresponding littermate controls were administered DOX intravenously. Survival curves were generated, and cardiac functions were measured in mice. The effects of TFEB on mitochondrial reactive oxygen species production, autophagic flux, and apoptosis were evaluated in human and mouse cardiac microvascular ECs treated with DOX. RNA sequencing, single-cell RNA sequencing, and chromatin immunoprecipitation with quantitative polymerase chain reaction was performed to dissect molecular mechanisms in DOX-treated ECs *in vitro* and *in vivo*. Mice with endothelium-specific deficiency of DAB adaptor protein 2 (*Dab2*) were subjected to measurement of cardiac function and fibrosarcoma growth under DOX treatment.

**RESULTS:** EC-specific TFEB transgenic mice showed significantly reduced mortality and improved cardiac function, together with attenuation of perivascular fibrosis after DOX treatment. By contrast, EC-specific TFEB knockout exacerbated DOX-induced cardiac dysfunction in mice. Furthermore, we observed that TFEB enhanced autophagy and reduced oxidative stress in cardiac microvascular ECs treated with DOX. In addition, TFEB preserved EC barrier integrity, alleviated proinflammatory cytokine release from cardiac microvascular ECs, and maintained the EC–cardiomyocyte communication, contributing to the protective effects of EC TFEB on cardiomyocyte function. Mechanistically, DAB2, a clathrin- and cargo-binding endocytic adaptor protein, was identified as a TFEB target gene in ECs. Accordingly, DAB2 knockdown attenuated the inhibitory effects of TFEB on apoptosis and the secretion of proinflammatory cytokines from cardiac microvascular ECs. *In vivo*, EC-specific *Dab2* deficiency abolished the protective effect of EC TFEB on DOX-induced cardiac dysfunction.

**CONCLUSIONS:** Taken together, endothelial TFEB protects against EC damage and cardiac dysfunction, constituting a potential target for treating cardiotoxicity induced by DOX. Our study provides new mechanistic insights into cardiotoxicity associated with chemotherapy.

**Key Words:** cardiotoxicity ■ chemotherapy ■ DAB2 ■ endothelial toxicity ■ transcription factor EB

Correspondence to: Yanbo Fan, MD, PhD, Department of Surgery, Division of Vascular Diseases and Surgery, Davis Heart and Lung Institute, College of Medicine, Wexner Medical Center, Ohio State University, 1645 Neil Ave, Columbia, OH 43210, Email fan.1411@osu.edu or Wa Du, MD, PhD, Department of Surgery, Division of Vascular Diseases and Surgery, Davis Heart and Lung Institute, College of Medicine, Wexner Medical Center, Ohio State University, 1645 Neil Ave, Columbia, OH 43210, Email du.1220@osu.edu

Supplemental Material is available at <https://www.ahajournals.org/doi/suppl/10.1161/CIRCULATIONAHA.124.071774>.

For Sources of Funding and Disclosures, see page XXX.

© 2026 American Heart Association, Inc.

*Circulation* is available at [www.ahajournals.org/journal/circ](http://www.ahajournals.org/journal/circ)

## Clinical Perspective

### What Is New?

- This study underscores the importance of preserving endothelial cell function as a pivotal strategy to alleviate the cardiotoxic effects of chemotherapeutic drugs.
- The study demonstrates endothelial TFEB (transcription factor EB) protects against doxorubicin-induced endothelial dysfunction and cardiotoxicity, constituting a potentially promising therapeutic approach to prevent or reduce cardiovascular toxicity.
- The study provides novel mechanistic insights into how endothelial TFEB mitigates doxorubicin-induced cardiotoxicity by preserving endothelial integrity.

### What Are the Clinical Implications?

- Enhancing endothelial TFEB function presents a potential therapeutic strategy to reduce cardiovascular toxicity in cancer patients receiving doxorubicin.
- Biomarker-based assessment of endothelial TFEB activity may support early risk stratification and tailored intervention for cancer patients at high risk of cardiotoxicity.
- Integration of endothelial TFEB-targeted approaches into oncological care has the potential to improve long-term cardiovascular outcomes and overall well-being for cancer survivors.

**D**oxorubicin (DOX) is an effective and widely used anthracycline for treating various cancers, including breast cancer, sarcoma, ovarian cancer, thyroid cancer, and small-cell lung cancer.<sup>1</sup> However, its long-term cardiac risks in cancer survivors are receiving increasing attention. Although numerous studies have revealed the adverse effects of DOX on cardiac function, most have focused on its direct impact on cardiomyocytes, leading to contractile dysfunction.<sup>2</sup> The crucial role of endothelial cells (ECs) in this pathological process remains largely underappreciated. ECs are the most abundant noncardiomyocyte cell type in both mice and humans, serving as a key physiological gatekeeper of cardiomyocytes during the infusion of antineoplastic agents.<sup>3,4</sup> DOX is administered intravenously into the systemic circulation, resulting in direct exposure of ECs to high concentrations of the drug. Recent clinical and preclinical research has demonstrated that DOX causes early and consistent endothelial dysfunction.<sup>5</sup> This EC dysfunction is thought to be triggered by systemic inflammation and vascular endothelial damage.<sup>6</sup> Therefore, preservation of EC function may represent a potential therapeutic avenue to prevent the development of DOX-induced cardiomyopathy.

## Nonstandard Abbreviations and Acronyms

<b>ANP</b>	atrial natriuretic peptide
<b>BNP</b>	brain natriuretic peptide
<b>CLDN11</b>	claudin-11
<b>DIC</b>	doxorubicin-induced cardiotoxicity
<b>DOX</b>	doxorubicin
<b>EC-Tfeb Tg</b>	endothelial cell–specific TFEB transgenic mouse
<b>EC</b>	endothelial cell
<b>FITC</b>	fluorescein isothiocyanate
<b>HCMEC</b>	human cardiac microvascular endothelial cell
<b>IL</b>	interleukin
<b>MCMEC</b>	mouse cardiac microvascular endothelial cell
<b>ROS</b>	reactive oxygen species
<b>scRNA-seq</b>	single-cell RNA sequencing
<b>TFEB</b>	transcription factor EB
<b>Tfeb<sup>ECKO</sup></b>	endothelial cell-selective TFEB knockout mouse
<b>WT</b>	wild-type

Unlike cardiomyocytes, ECs from the adult heart can proliferate, migrate, and sprout, highlighting the potential of ECs in the “response to damage” and indicating that ECs may serve as a potential therapeutic target for cardiac disease induced by chemotherapeutic drugs.<sup>7</sup> The endothelial toxicity induced by DOX is a multifaceted response involving multiple mechanisms, including disruption of DNA repair mediated by TOP2B (topoisomerase IIβ),<sup>8</sup> oxidative stress,<sup>9</sup> inflammation,<sup>6</sup> and consequent mitochondrial dysfunction.<sup>10</sup> As a critical process for degrading and recycling damaged organelles or cellular components, proper autophagic flux is essential to maintain the physiological functions of ECs.<sup>11</sup> Autophagy is enhanced to ensure cell survival under mild cellular stress. However, when cellular stress is overwhelming, autophagy cannot remove damaged and detrimental cell components, resulting in autophagic cell death.

TFEB (transcription factor EB) controls autophagy, lysosome biogenesis, and lysosomal exocytosis. As a transcription factor, TFEB binds to a conserved DNA element known as the CLEAR box in the promoter of target genes.<sup>12</sup> Accumulating evidence indicates that TFEB is essential for maintaining vascular homeostasis. Our previous studies have demonstrated that endothelial TFEB inhibits oxidative stress, improves systemic insulin sensitivity, and promotes postischemic blood flow recovery in mice.<sup>13,14</sup> However, the role of EC TFEB in cardiotoxicity induced by DOX remains unclear. This study aims to determine whether TFEB in ECs can prevent DOX-induced endothelial damage and alleviate cardiac dysfunction. We

present comprehensive analyses exploring the role and mechanisms through which EC TFEB protects against cardiotoxicity under DOX treatment. Better mechanistic insight into the chemotherapy-induced EC damage would provide novel therapeutic targets to prevent cardiotoxicity associated with cancer treatment.

## METHODS

### Data Availability

Sequencing data have been deposited in the Gene Expression Omnibus under accession numbers GSE237200 and GSE285475. All supporting data are available from the corresponding author upon reasonable request. A major resources table and detailed methods are provided in the [Supplemental Material](#).

### Animals and Experimental Design

All animal experiments were performed under a protocol approved by the University of Cincinnati institutional animal care and use committee (No. 22-09-23-01), in accordance with the Animal Research: Reporting of In Vivo Experiments (ARRIVE) guidelines and the *Guide for the Care and Use of Laboratory Animals* (National Institutes of Health publication No. 85-23, revised 2011).

To investigate the role of TFEB in endothelial cells, we used EC-specific TFEB transgenic (EC-*Tfeb* Tg) and conditional knockout (*Tfeb*<sup>ECKO</sup>) mice ([Supplemental Methods](#)). All mice were maintained under standard conditions (a 12-hour light/dark cycle) with ad libitum access to food and water, and were fed a regular diet (LabDiet 5053; 24.5% protein, 13.1% fat, 62.4% carbohydrate). Mice were euthanized by carbon dioxide asphyxiation at designated end points. In humans, cumulative DOX doses of 700 mg/m<sup>2</sup> result in an exponential increase in DOX-induced cardiotoxicity (DIC) rates of up to 48%,<sup>15</sup> equivalent to 18.9 mg/kg in mice. A standard model of chronic myocardial injury was used in this study. DOX-based chemotherapy is standard first-line treatment for patients with soft tissue sarcoma.<sup>16</sup> Epidemiological studies have reported a higher incidence of sarcoma and fibrosarcoma in human males compared with females.<sup>17–19</sup> Therefore, male mice with or without sarcoma burden were used in the current studies. Briefly, 8- to 10-week-old male mice, including EC-*Tfeb* Tg, littermate wild-type (WT), *Tfeb*<sup>ECKO</sup>, and littermate *Tfeb*<sup>f/f</sup>, were intravenously administered DOX (5 mg/kg/wk for 5 weeks). Survivability was determined up to 8 weeks after the first DOX dose. Eight- to ten-week-old male WT and EC-*Tfeb* Tg mice were administered AAV2-QuadYF virus (VectorBuilder Inc.), which transduces either EGFP-shScramble or EGFP-shmDab2 (1×10<sup>11</sup> genome copies/mouse intravenously). Three weeks later, the mice were subcutaneously injected with MCA205 cells (2×10<sup>5</sup> cells/mouse), a mouse fibrosarcoma cell line, and received DOX treatment (5 mg/kg/wk for 5 weeks intravenously). Tumor growth was monitored, and cardiac function was assessed both before and after DOX treatment. Only mice with confirmed fibrosarcoma growth were included for DOX treatment and subsequent assessment of cardiac function. Mice displaying significant weight loss (>20%) or severe organ dysfunction were excluded from the study.

### Statistical Analysis

All quantitative data represent individual data points. Unless otherwise stated, values are presented as mean±SEM. N represents the number of individual mice or independent biological replicates as specified in the figure legends. Before analysis, all data were tested for normality and homogeneity of variance. The Student *t* test (unpaired *t* test) was used for 2 groups, whereas 1-way ANOVA, 2-way ANOVA, or 2-way mixed ANOVA, followed by an appropriate post hoc test (Tukey post hoc test), was used for comparing >2 groups. Kaplan-Meier survival curves for WT, EC-*Tfeb* Tg, *Tfeb*<sup>f/f</sup>, and *Tfeb*<sup>ECKO</sup> mice were compared using the log-rank test. *P* values were calculated using GraphPad Prism 10.1.0 software, and the statistical significance was considered at *P*<0.05. Asterisks in the figures indicate statistical significance as follows: \**P*<0.05; \*\**P*<0.01; \*\*\**P*<0.001.

## RESULTS

### Endothelial TFEB Reduces Mortality, Preserves Cardiac Function, and Attenuates Perivascular Fibrosis in Mice Treated With DOX

To investigate the role of EC TFEB in vascular EC damage and cardiac dysfunction induced by DOX, we used EC-*Tfeb* Tg, *Tfeb*<sup>ECKO</sup>, and corresponding littermate control mice subjected to DOX treatment. EC-*Tfeb* Tg (n=20) and WT (n=26) mice were administered DOX at a dose of 5 mg/kg/wk for 5 weeks by tail vein injection, resulting in a cumulative dose of 25 mg/kg. The Kaplan-Meier survival curve was generated for WT and EC-*Tfeb* Tg mice after DOX administration (Figure 1A). The EC-*Tfeb* Tg significantly increased mouse survival. Cardiac function was monitored by transthoracic echocardiography at baseline (week 0) and 8 weeks after DOX treatment. In the WT group, DOX treatment reduced ejection fraction (41.5%) and fractional shortening (20.6%) compared with baseline (ejection fraction, 55.1%; fractional shortening, 28.4%), whereas the cardiac function was significantly preserved in EC-*Tfeb* Tg mice (Figure 1B; [Figure S1A](#)), suggesting that EC TFEB transgene protects against DOX-induced cardiac dysfunction. Perivascular fibrosis, an early stage of cardiac fibrosis, and interstitial myocardial fibrosis are typical histological phenotypes in DIC.<sup>20</sup> To quantify the extent of fibrosis induced by DOX, sequential staining of continuous heart tissue sections with hematoxylin-eosin (Figure 1C), Masson's trichrome (Figure 1D), and picrosirius red (Figure 1E) was performed to visualize collagen accumulation. EC-*Tfeb* Tg mice exhibited significantly reduced perivascular fibrosis (Figure 1D; Tg, 15.5% versus WT, 39.9%) and overall collagen deposition (Figure 1E, including both perivascular and interstitial fibrosis). To evaluate the impact of EC TFEB on heart failure induced by DOX, we measured the expression of ANP (atrial natriuretic peptide) and BNP (brain natriuretic peptide) *in vivo*, along with pulmonary and hepatic congestion potentially resulting from heart failure. EC-*Tfeb* Tg significantly reduced BNP and ANP levels in heart tissues ([Figure S1B](#)) after validation of serum BNP

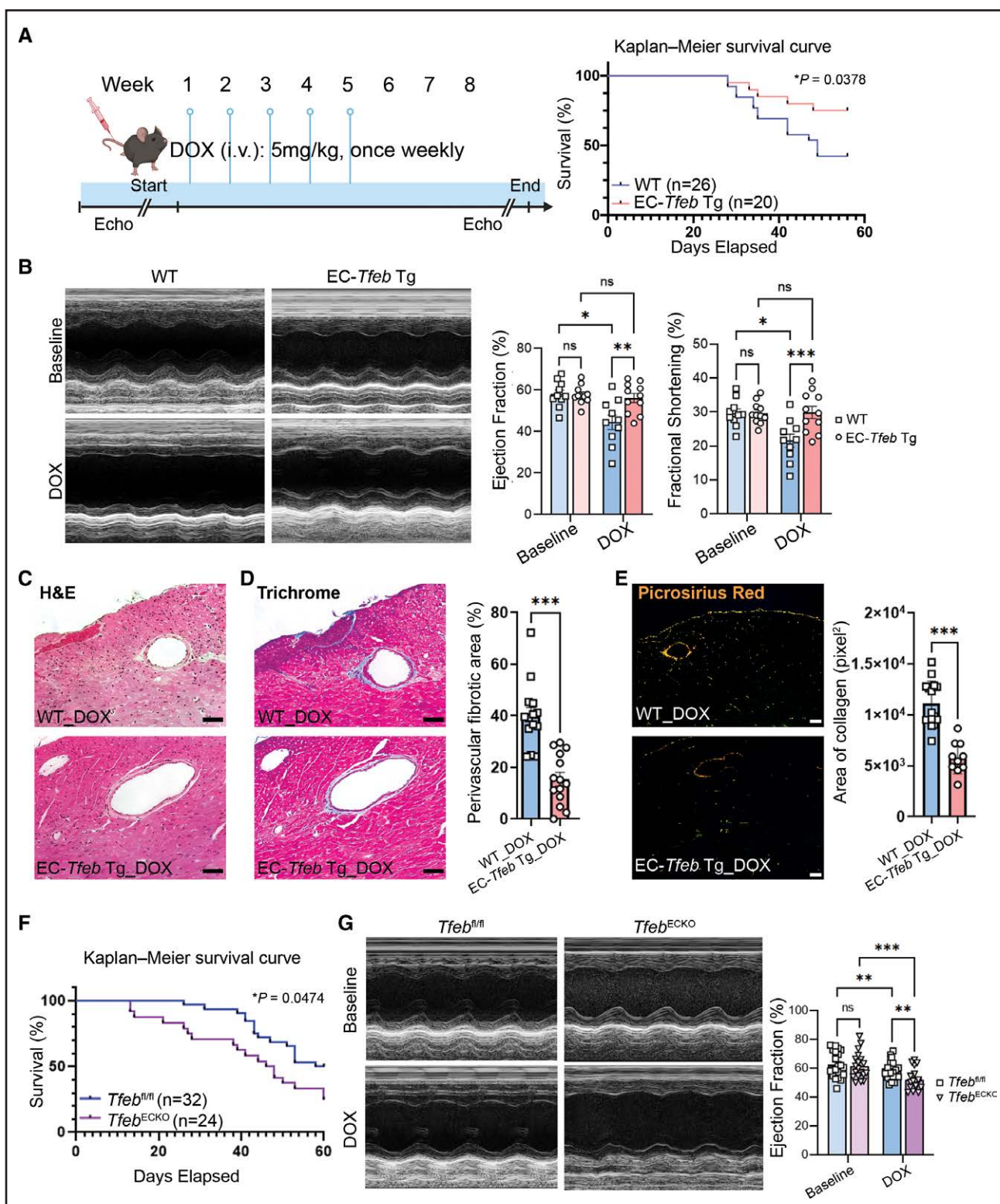


**Figure 1. Endothelial TFEB prevents cardiac dysfunction and attenuates perivascular fibrosis in mice treated with DOX.**

**A**, A schematic illustration of the in vivo model used to evaluate DOX-induced chronic cardiotoxicity. Male wild-type (WT) and EC-Tfeb Tg mice were injected with DOX (5 mg/kg IV) once weekly for 5 weeks, for a cumulative dose of 25 mg/kg. Kaplan–Meier survival curves of DOX-treated mice (WT, n=26; EC-Tfeb Tg, n=20; log-rank test P=0.0378). **B**, Representative 2D M-mode echocardiograms of WT and EC-Tfeb Tg mice were obtained at baseline and 8 weeks after DOX treatment. Ejection fraction and fractional shortening were quantified (n=10 or 11 per group). **C** through **E**, Representative hematoxylin–eosin (H&E) staining (**C**), Masson’s trichrome staining (**D**), and picrosirius red staining (**E**) of continuous paraffin sections from DOX-treated animals. Collagen content (from Masson’s trichrome and picrosirius red staining) was quantified. n=14 per group (**D**) and n=10 to 15 per group (**E**). Scale bar=100 µm. **F**, Kaplan–Meier survival curves of Tfeb<sup>fl/fl</sup> and Tfeb<sup>ECKO</sup> mice are shown (Continued)

**Figure 1 Continued.** (*Tfeb<sup>fl/fl</sup>*, n=32; *Tfeb<sup>ECKO</sup>*, n=24; log-rank test  $P=0.0474$ ). **G**, Representative M-mode echocardiograms of *Tfeb<sup>fl/fl</sup>* and *Tfeb<sup>ECKO</sup>* mice were obtained at baseline and 6 weeks after DOX treatment (5 mg/kg IV, once weekly for 4 weeks; cumulative dose 20 mg/kg). Ejection fraction was assessed and analyzed (n=19 or 20 per group). A log-rank test was used for survival analysis in **A** and **F**. Two-way mixed ANOVA followed by Tukey post hoc test was used in **B** and **G**. An unpaired *t* test was used in **D** and **E**. Data are presented as mean±SEM; \* $P<0.05$ , \*\* $P<0.01$ , \*\*\* $P<0.001$ .

under DOX treatment conditions (Figure S1C). We observed reduced vascular congestion and fibrosis in the lungs of EC-*Tfeb* Tg mice treated with DOX (Figure S2A and S2B), indicating reduced chronic pulmonary congestion compared with WT mice. In the liver of our DOX-treated mouse models, we observed mild congestion, and no significance was detected (Figure S2C). To test whether EC TFEB is essential for protection against DOX-induced cardiac dysfunction, we used *Tfeb<sup>ECKO</sup>* mice in the DOX model. In contrast with the protective effects observed in EC-*Tfeb* Tg mice, EC TFEB deficiency worsened DOX-induced mortality (Figure 1F). *Tfeb<sup>ECKO</sup>* further exacerbated cardiac dysfunction, as evidenced by decreased ejection fraction, fractional shortening, and left ventricular posterior wall thickness at systole, along with increased left ventricular internal diameter at systole (Figure 1G; Figure S3A and S3B). In addition, *Tfeb<sup>ECKO</sup>* mice consistently exhibited elevated BNP and ANP levels (Figure S3C and S3D). *Tfeb<sup>ECKO</sup>* mice also displayed increased vascular congestion and fibrosis in the lungs compared with control mice (Figure S4A and S4B). However, *Tfeb<sup>ECKO</sup>* did not significantly affect liver congestion (Figure S4C). To validate EC-*Tfeb* Tg or knockout in our mouse models, we isolated mouse cardiac microvascular endothelial cells (MCMECs) and characterized them with immunostaining for CD31 and VE-cadherin (Figure S5A). Western blot analysis indicated that TFEB expression was increased 1.8-fold in EC-*Tfeb* Tg mice and reduced to 16% in *Tfeb<sup>ECKO</sup>* mice compared with the corresponding control mice (Figure S5B and S5C). Compared with *Tfeb<sup>fl/fl</sup>* control, *Tfeb<sup>ECKO</sup>* did not affect TFEB expression in nonendothelial heart tissue cells (Figure S5D). Indeed, our data suggest that TFEB expression is significantly reduced by DOX treatment at the indicated doses in primary human cardiac microvascular endothelial cells (HCMECs) and MCMECs (Figure S6A and S6B). However, the nuclear content of TFEB was significantly increased at 8 hours and 24 hours after DOX treatment, indicating that cellular stress induces TFEB nuclear translocation (Figure S6C). Taken together, TFEB is responsive to DOX treatment in cardiac microvascular endothelial cells, and EC TFEB protects against vascular damage and cardiac dysfunction under DOX treatment conditions.

## TFEB Inhibits DOX-Induced EC Apoptosis and Reduces DOX-Induced Reactive Oxygen Species Production

DOX induces EC apoptosis, reduces capillary density, and increases microvascular permeability in the heart.<sup>21</sup> The apoptotic ECs were detected by TUNEL staining and immunostaining for CD102 (ICAM-2), an EC marker. Com-

pared with the control group, the EC-*Tfeb* Tg did not affect vascular density in mouse heart tissues under vehicle control conditions. However, it preserved vascular density and reduced EC apoptosis in mouse heart tissues treated with DOX (Figure 2A). The effect of TFEB on EC apoptosis was evaluated by flow cytometry using Annexin V and 7-aminoactinomycin D staining. MCMECs from EC-*Tfeb* Tg mice exhibited decreased apoptosis compared with controls under normal conditions (6.3% versus 15.8%) and DOX treatment conditions (51.9% versus 69.8%; Figure 2B). Moreover, EC-*Tfeb* Tg inhibited caspase-3 activity in MCMECs (Figure 2C). Similar results of Annexin V staining were observed in TFEB-overexpressing human ECs (Figure 2D; Figure S7A). Consistently, the loss of TFEB in HCMECs increased apoptosis under both normal and DOX-treated conditions (Figure 2E; Figure S7B and S7C). The efficiency of TFEB knockdown was validated in HCMECs (Figure S7D). To uncover the mechanisms by which TFEB protects EC function, we conducted RNA sequencing analysis on the stable TFEB overexpressing human umbilical vein ECs and control ECs in the presence or absence of DOX (Figure S8). The differential gene expression and pathway enrichment analysis indicated that multiple pathways, including inflammatory response, apoptosis, and IL (interleukin)-6 signaling, were enriched in control ECs compared with TFEB-overexpressing ECs under DOX treatment (Figure 2F). The pathway enrichment plot showed that DOX treatment upregulates the apoptosis pathway (Figure 2G), and TFEB overexpression significantly inhibits this pathway (Figure 2H).

Excessive generation of mitochondrial reactive oxygen species (ROS) is one of the primary causes of DOX-induced EC dysfunction. HCMECs and MCMECs were treated with DOX, and mitochondrial ROS production was measured by flow cytometry using MitoSOX (Figure S9). TFEB overexpression significantly reduced the median fluorescence intensity (of mitochondrial ROS in cardiac microvascular endothelial cells treated with DOX (Figures 2I and 2J). TFEB knockdown consistently increased ROS production (Figure 2K), suggesting an essential role of TFEB in attenuating ROS when ECs are treated with DOX. Taken together, we demonstrated that TFEB inhibits apoptosis and ROS production in cardiac microvascular endothelial cells under DOX treatment conditions.

## TFEB Restricts IL-6 and IL-1 $\beta$ Release From ECs

Through RNA sequencing analysis, we identified multiple signaling pathways in response to DOX (Figure S10A), with the inflammatory response playing a critical role in

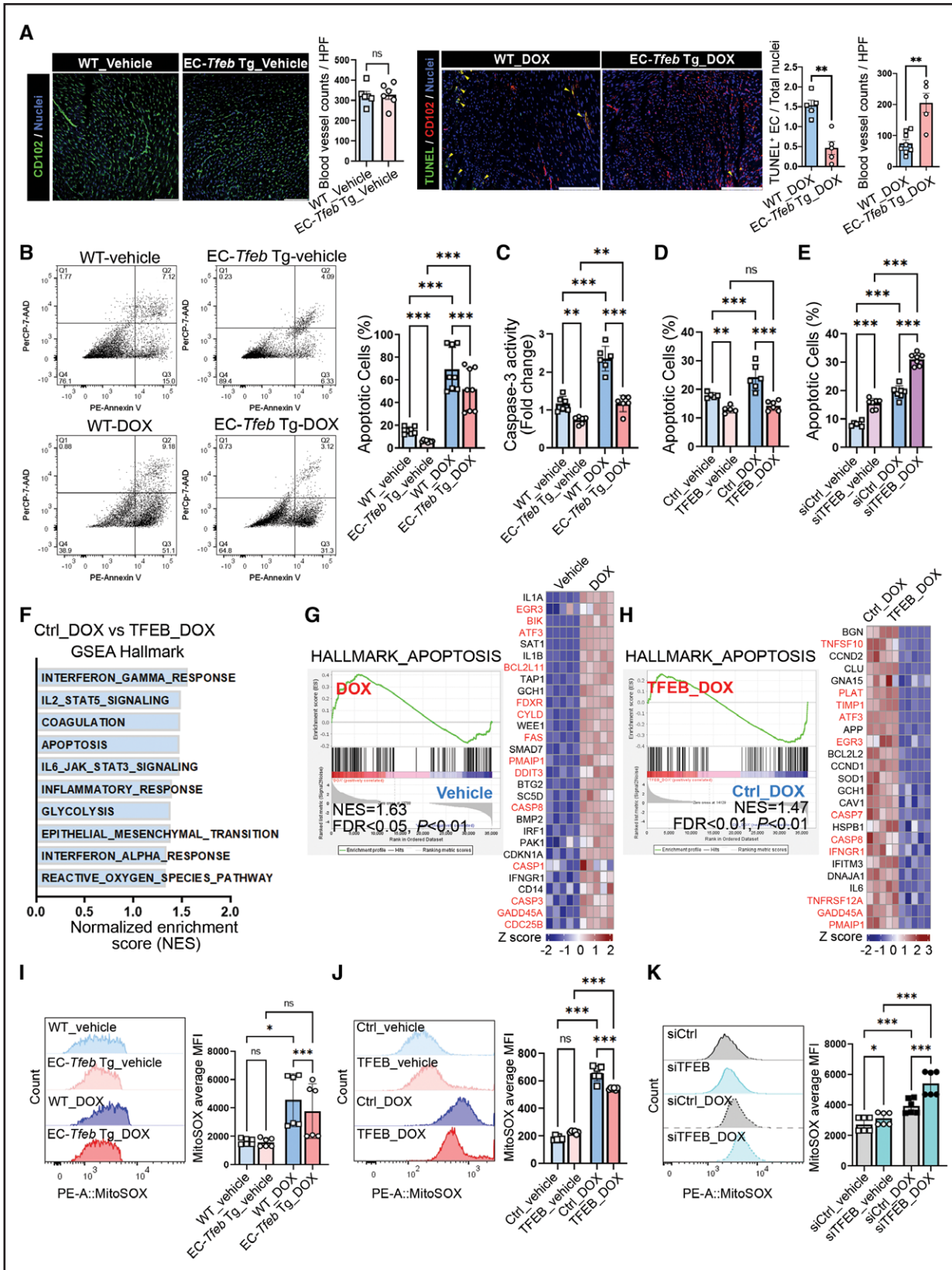


**Figure 2.** TFEB ameliorates DOX-induced endothelial apoptosis and protects against ROS production.

**A**, Wild-type (WT) and EC-*Tfeb* Tg mice were treated with vehicle or DOX (5 mg/kg IV) once weekly for 5 weeks, for a cumulative dose of 25 mg/kg. At the end point (8 weeks after initial DOX treatment), vascular density was assessed by immunostaining CD102, an EC marker. Endothelial apoptosis was evaluated by TUNEL and CD102 (red) double staining, with apoptotic ECs indicated by yellow arrowheads. Apoptotic ECs and vascular density (vessels/HPF) were quantified and statistically analyzed ( $n=5-8$  per group). Scale bar=100  $\mu$ m. (Continued)

**Figure 2 Continued.** **B**, Mouse cardiac microvascular endothelial cells (MCMECs) isolated from WT and EC-*Tfeb* Tg mice were treated with DOX (1  $\mu$ M) or vehicle for 24 hours. Apoptosis was assessed by flow cytometry using Annexin V and 7-AAD ( $n=8$ ). **C**, Caspase-3 activity was determined using a Caspase-3 Assay Kit ( $n=6$ ). **D**, HUVECs stably overexpressing TFEB or control (Ctrl) ECs were generated using retrovirus transduction. ECs were treated with vehicle or DOX (1  $\mu$ M) for 24 hours. Apoptotic cells were determined by flow cytometry analysis of Annexin V and 7-AAD ( $n=5$  or 6). **E**, Human cardiac microvascular endothelial cells (HCMECs) were transfected with control siRNA (siCtrl) or siRNA targeting TFEB (siTFEB; 20 nM) for 48 hours, followed by treatment with DOX (1  $\mu$ M) for 24 hours. Apoptosis was measured by flow cytometry using Annexin V and 7-AAD staining ( $n=6$  or 7). **F**, RNA sequencing analysis was performed on HUVECs stably overexpressing TFEB or Ctrl, treated with vehicle or DOX (1  $\mu$ M) for 24 hours. Pathway analysis was conducted on differentially upregulated genes (Ctrl\_DOX vs TFEB\_DOX). **G** and **H**, Gene Set Enrichment Analysis (GSEA) enrichment plots for the HALLMARK\_APOPTOSIS pathway were generated by comparing Ctrl\_DOX vs Ctrl\_vehicle and TFEB\_DOX vs Ctrl\_DOX. Corresponding heatmaps display differentially expressed genes (DEGs), in which proapoptotic genes are highlighted in red. The Z score below each heatmap represents the number of standard deviations the expression level of a gene deviates from the mean across all samples, indicating relative upregulation or downregulation.  $n=5$  per group in **F** through **H**. **I**, MCMECs from WT and EC-*Tfeb* Tg mice were treated with DOX (1  $\mu$ M) for 8 hours, followed by incubation with MitoSOX (5  $\mu$ M) for 30 min. ROS production was measured by flow cytometry, and the median fluorescent density (MFI) of MitoSOX was quantified for each group ( $n=6$ ). **J**, ROS production was measured by flow cytometry analysis of MitoSOX in HUVECs stably overexpressing TFEB or Ctrl ECs treated with DOX (1  $\mu$ M) for 8 hours ( $n=6$ ). **K**, HCMECs were transfected with siCtrl or siTFEB (20 nM) for 48 hours, then incubated with MitoSOX (5  $\mu$ M) for 30 min. ROS production was evaluated by flow cytometry ( $n=6$ ). An unpaired *t* test was used in **A**. Data in **B** through **E** and **I** through **K** were analyzed by 2-way ANOVA followed by Tukey post hoc test. Data are presented as mean  $\pm$  SEM; \* $P<0.05$ , \*\* $P<0.01$ , \*\*\* $P<0.001$ . FDR indicates false discovery rate; and NES, normalized enrichment score.

DOX-induced EC dysfunction and potential intercellular communication. TFEB mitigated the effects of DOX on inflammatory response and IL-6 signaling pathways (Figure S10B through S10E). The volcano plot highlights the genes involved in the inflammatory response induced by DOX (Figure 3A, left), whereas TFEB overexpression decreased the expression of these proinflammatory genes in ECs (Figure 3A, right). Pathway enrichment analysis further revealed that TFEB attenuated *NABA\_SECRETED\_FACTORS* enrichment in ECs treated with DOX (Figure 3B). Pathways related to cytokine activity and chemoattractant signaling were enriched in control ECs but not in the TFEB-overexpressing ECs (Figure 3C). A heatmap illustrated the downregulated inflammatory response-associated genes in the TFEB-overexpressing ECs treated with DOX (Figure 3D). The top DOX-upregulated proinflammatory genes (IL6, IL1B, CCL2, CCL20, CCL5) were downregulated by TFEB in human ECs (Figure 3E). In MCMECs with the *Tfeb* transgene, the expression of *Il6* and *Il1b* was reduced compared with control ECs (Figure S11A). In EC-*Tfeb* Tg mice, both mRNA and protein levels of IL-6 and IL-1 $\beta$  were reduced in the cardiac tissue compared with controls (Figure S11B through S11D). Conversely, *Tfeb*<sup>ECKO</sup> led to increased levels of IL-6 and IL-1 $\beta$  in heart tissues (Figure S12A through S12C). These results suggest that EC TFEB restricts the inflammatory response in ECs and heart tissues triggered by DOX treatment.

## TFEB Alleviates DOX-Induced Autophagosome Accumulation and Upregulates Lysosome and Endocytosis Pathways

TFEB plays a crucial role in autophagy and lysosomal function. DOX treatment increased the Pearson correlation coefficients between LC3 and Lysotracker in control human ECs, but not in TFEB-overexpressing ECs, suggesting that TFEB overexpression inhibits DOX-induced

autophagosome accumulation in ECs (Figure 4A). Similarly, the EC-*Tfeb* Tg was able to reduce autophagosome accumulation in MCMECs under DOX treatment (Figure 4B). To quantify autophagic flux in ECs, we generated HUVECs stably overexpressing mCherry-EGFP-LC3B. Ratiometric analysis revealed that DOX treatment significantly increased the mCherry/GFP ratio with quenched GFP fluorescence (Figure S13A through S13D), suggesting that DOX increases autophagic flux but impairs autolysosome function (as reflected by increased red fluorescence signal). Increased autophagic flux, as determined by the ratiometric analysis, was consistent with the determination by the LC3-II/LC3-I ratio measured by Western blotting (Figure S13E through S13G), a conventional method for autophagic flux. DOX treatment alone increased LC3B-II/LC3B-I, and after adding Baflomycin A1, an autophagosome-lysosome fusion inhibitor,<sup>22</sup> LC3-II/LC3-I further increased, indicating DOX induces the autophagic flux (Figure S13F and S13G). TFEB deficiency exacerbated autolysosome dysfunction under DOX treatment (Figure 4C). Our RNA sequencing analysis revealed that the gene set associated with Positive Regulation of Autophagy was enriched in DOX-treated ECs, although the difference was not statistically significant (Figure S13H). TFEB overexpression upregulates lysosome (Figure 4D) and endocytosis pathways (Figure 4E). The upregulation of genes related to lysosomal and endocytic functions, including DNASE2, ARSG, CLTCL1, CORO1A, HPS4, and NAGLU, was validated by quantitative polymerase chain reaction (Figure 4F). Taken together, TFEB reduces autophagosome accumulation by enhancing autolysosome function in ECs treated with DOX.

## TFEB Attenuates IL-1 $\beta$ and IL-6 Release by Upregulation of DAB2 in ECs

To uncover novel TFEB target genes in response to DOX treatment, we performed a Venn diagram analysis

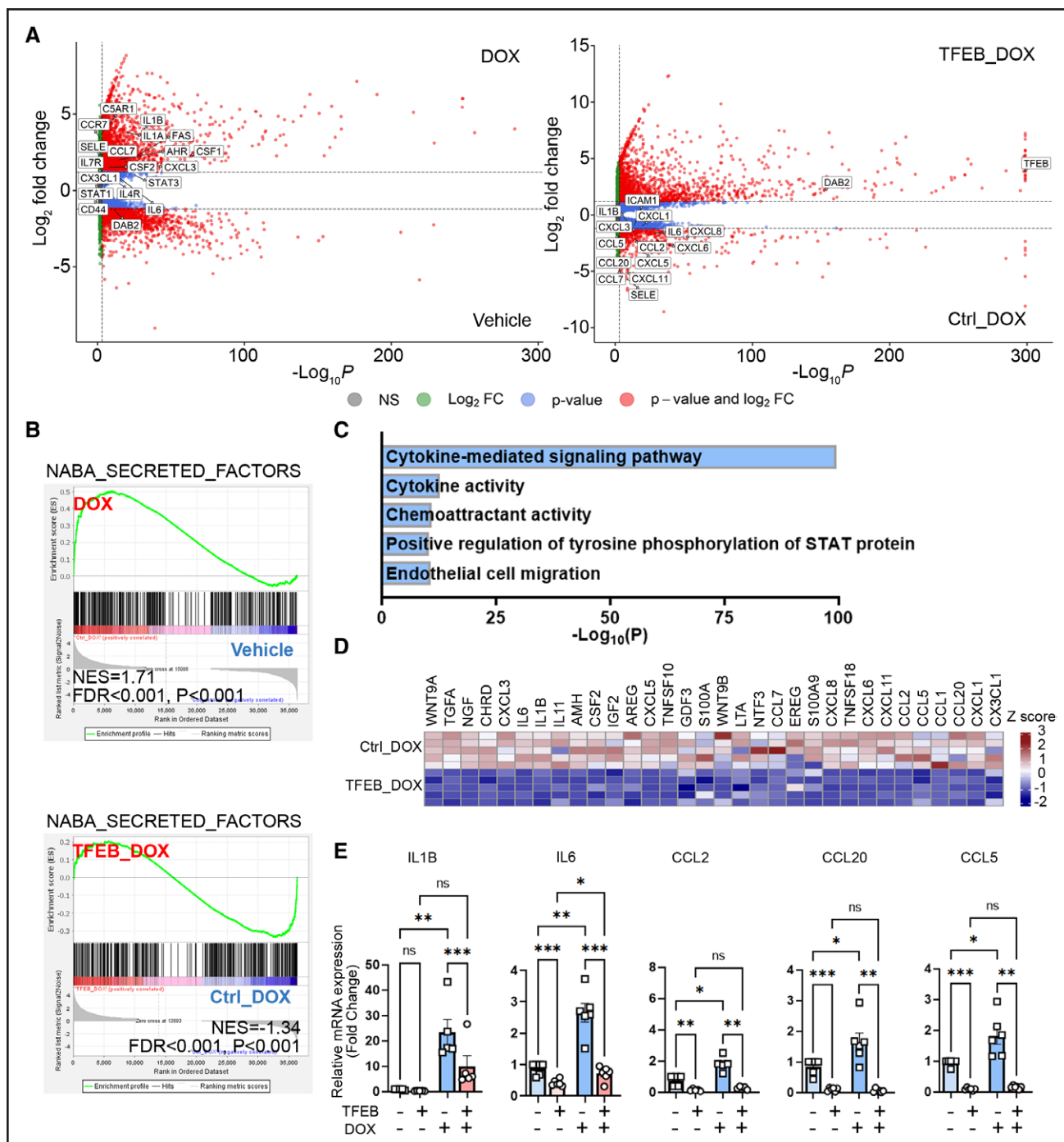


**Figure 3. TFEB restricts DOX-induced IL-6 and IL-1 $\beta$  release from ECs.**

**A**, Volcano plot showing log<sub>2</sub> fold change (y axis) and -log<sub>10</sub> adjusted P value (x axis). Genes with P<0.05 are shown in blue, those with an absolute log<sub>2</sub> fold change >1 are shown in green, and genes meeting both criteria (P<0.05 and absolute log<sub>2</sub> fold change >1) are shown in red. P values were adjusted for multiple comparisons using the false discovery rate (FDR) method in the DESeq2 package. Inflammation-related genes are highlighted. **B**, The NABA\_SECRETED\_FACTORS gene set was enriched in the DOX group and attenuated in the TFEB\_DOX group compared with the Ctrl\_DOX group. **C** and **D**, Multiple cytokine signaling pathways were enriched in DOX group (**C**), and a heatmap shows secreted cytokines that were downregulated in the TFEB\_DOX group (**D**). n=5 per group in **A** through **D**. **E**, The top-regulated proinflammatory genes were validated by quantitative polymerase chain reaction (qPCR) in HUVECs stably expressing TFEB or control ECs treated with vehicle or DOX (1  $\mu$ M) for 24 hours (n=5 or 6). Data in **E** were analyzed by 2-way ANOVA followed by Tukey post hoc test. Data are presented as mean $\pm$ SEM; \*P<0.05, \*\*P<0.01, \*\*\*P<0.001.

integrating 4 different gene sets: upregulated genes by TFEB overexpression in ECs treated with vehicle (3267 genes), upregulated genes by TFEB overexpres-

sion in ECs treated with DOX (3370 genes), a TFEB chromatin immunoprecipitation sequencing dataset using HUVECs (GSE88894, 1002 genes),<sup>23</sup> and genes

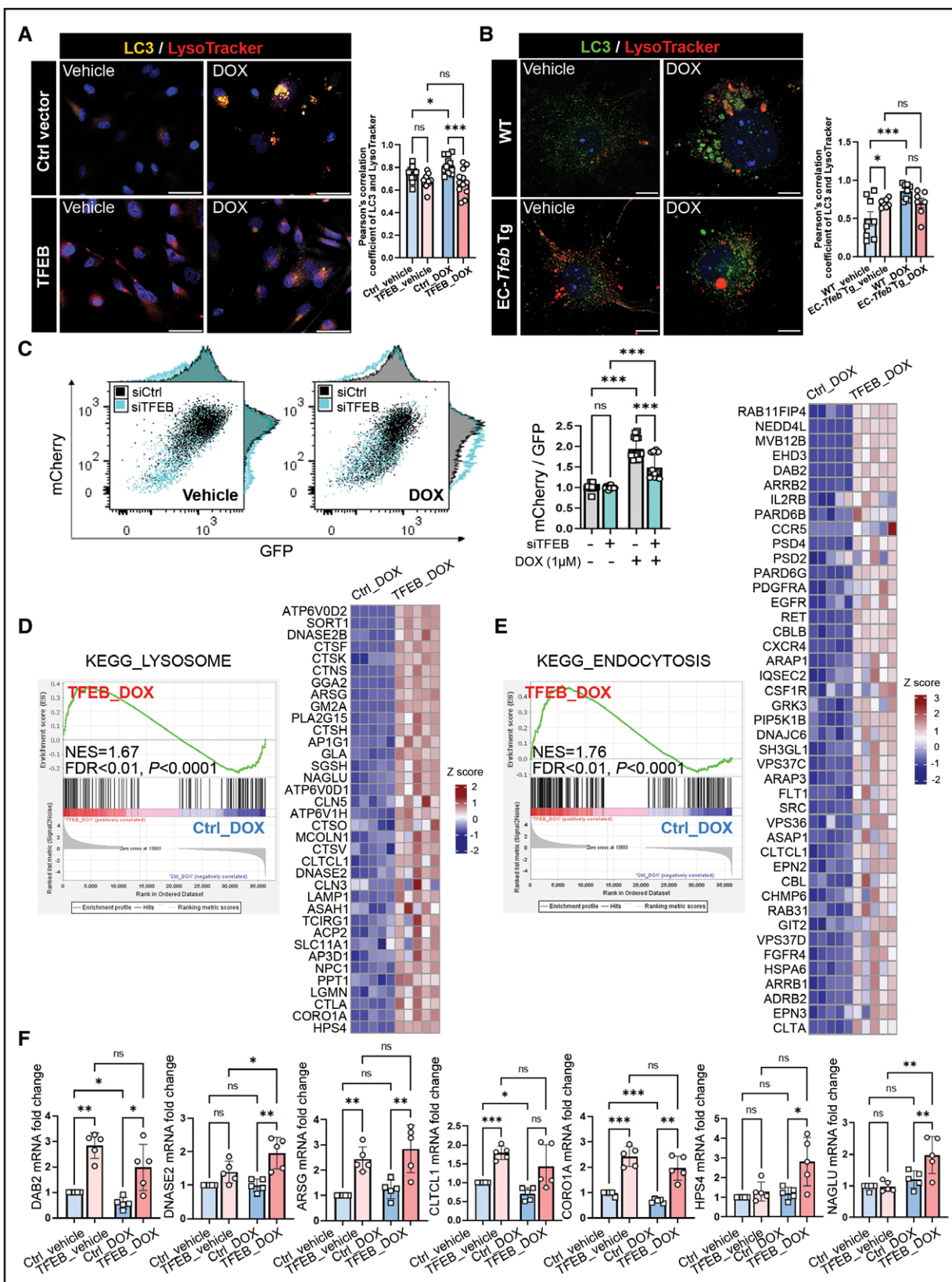


**Figure 4. TFEB reduces DOX-induced autophagosome accumulation.**

**A** and **B**, HUVECs stably overexpressing TFEB and control ECs (**A**), and MCMECs from wild-type and EC-*Tfeb* Tg mice (**B**), were treated with either vehicle or DOX (1  $\mu$ M) for 24 hours, followed by incubation with Lysotracker (50 nM, red) for 4 hours. Cells were immunostained for LC3 (gold). Pearson correlation coefficients of LC3 and Lysotracker colocalization were used to assess the intensity correlation between LC3 and lysosomes, analyzed using ImageJ.  $n=10$  to 12 per group, scale bar=20  $\mu$ m in **A**;  $n=7$  or 8 per group, scale bar=50  $\mu$ m in **B**. (Continued)

**Figure 4 Continued.** **C**, HUVECs stably expressing mCherry-EGFP-LC3 (C-G-LC3-EC) were transfected with either siCtrl or siTFEB (20 nM) for 48 h, followed by DOX (1 μM) treatment for 24 hours. Representative ratiometric flow cytometry images of autophagic flux are shown (**left**), and quantification of autophagic flux (mCherry/GFP) in ECs is shown on the **right** (n=12). **D**, GSEA enrichment plot of the KEGG\_LYSOSOME pathway comparing TFEB\_DOX to Ctrl\_DOX. **E**, GSEA enrichment plot of the KEGG\_ENDOCYTOSIS pathway comparing TFEB\_DOX to Ctrl\_DOX. n=5 per group in **D** and **E**. **F**, Lysosome- and endocytosis-related genes were validated by quantitative polymerase chain reaction (qPCR; n=5). Data in **A** through **C** and **F** were analyzed by 2-way ANOVA followed by Tukey post hoc test. Data are presented as mean±SEM; \*P<0.05, \*\*P<0.01, \*\*\*P<0.001.

involved in the autophagosome-lysosomal pathway (891 genes).<sup>24</sup> Our analysis revealed that DAB2 is one of the 11 TFEB candidate target genes and the most highly upregulated among them (Figure 5A). TFEB increased DAB2 expression at the mRNA level in HUVECs (Figure 4F). Reanalysis of chromatin immunoprecipitation sequencing data revealed potential TFEB binding sites in the promoter of human DAB2 (Figure 5B). TFEB binding to the DAB2 promoter was validated by chromatin immunoprecipitation with quantitative polymerase chain reaction (Figure 5C). We also found that TFEB activates DAB2 promoter activity measured by a luciferase reporter assay using constructs with or without DAB2 promoter sequences (Figure 5D). Similar to TFEB, DOX treatment led to a dose-dependent downregulation of DAB2 in MCMECs and HCMECs (Figure S14A and S14B). TFEB knockdown decreased DAB2 protein expression in HCMECs (Figure 5E). Consistently, the TFEB transgene led to a 2.8-fold increase in DAB2 protein expression in MCMECs (Figure 5F), and stable TFEB overexpression increased DAB2 expression by approximately 4.9-fold (Figure 5G). These data suggest that DAB2 is responsive to DOX treatment and is a target gene of TFEB. To examine whether DAB2 regulates ROS production, autophagic flux, and apoptosis in ECs, we performed flow cytometry of MitoSOX, ratiometric flow cytometry analysis of mCherry/GFP in mCherry-EGFP-LC3B-expressing endothelial cells, and Annexin V apoptosis assays. Our results showed that DAB2 knockdown significantly increased ROS production (Figure 5H) and impaired autolysosome formation and autophagic flux (Figure 5I). To examine whether DAB2 mediates TFEB-dependent protective effects on EC function, we performed DAB2 silencing using small interfering RNA in TFEB-overexpressing ECs (Figure S14C). The results indicated that DAB2 knockdown abolished the inhibitory effects of TFEB on IL-6 and IL-1β release and apoptosis in ECs treated with DOX (Figure 5J and 5K; Figure S15). Collectively, DAB2 is a TFEB target gene and is essential for TFEB-mediated protection against EC dysfunction under DOX treatment.

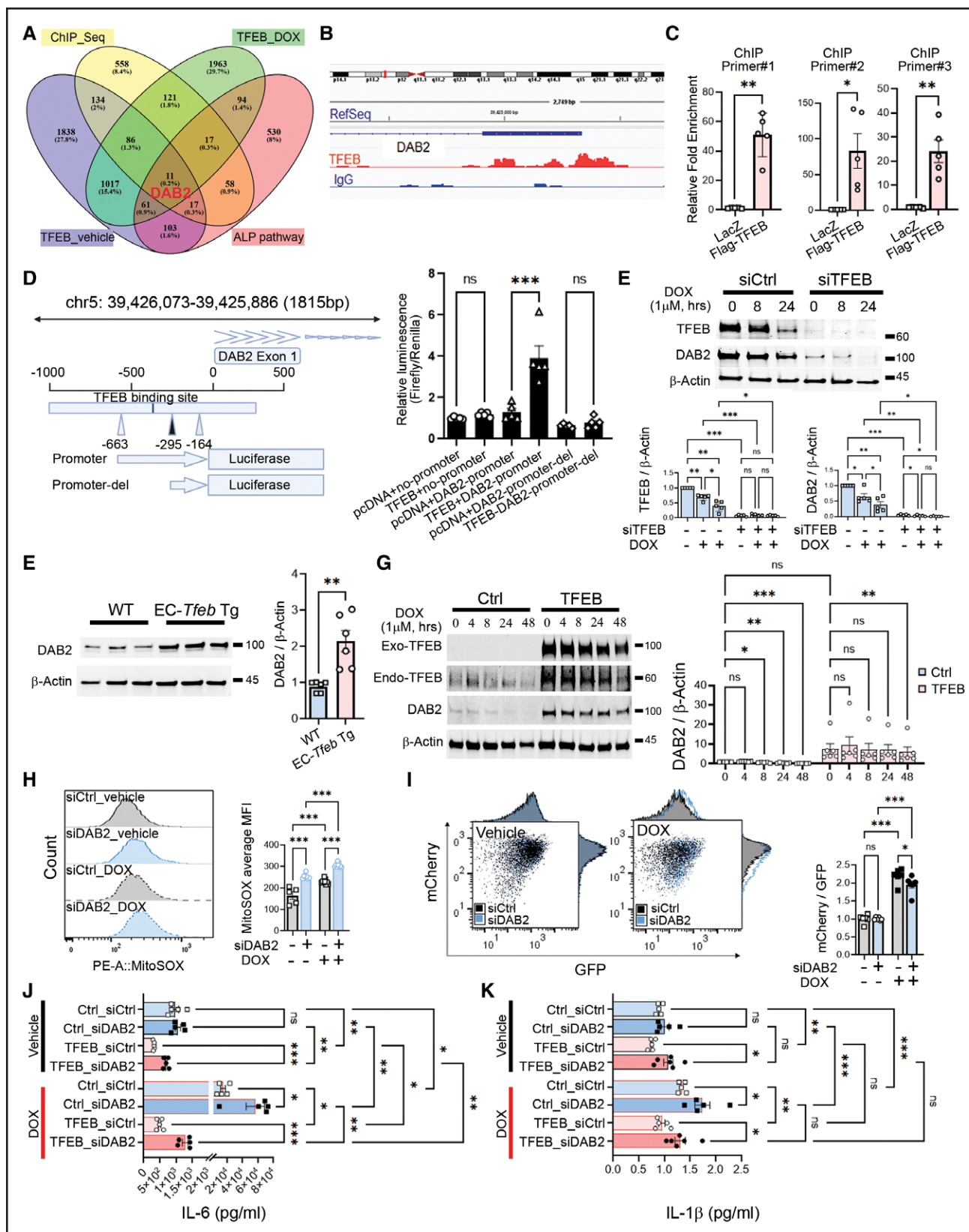
## TFEB Inhibits DOX-Induced EC Damage by Modulating Multiple Signaling Pathways in Vivo

The early asymptomatic stages of DIC are challenging to detect by cardiac imaging alone, and the initiating

mechanisms are incompletely understood. To explore the mechanisms mediating the protective effects of EC TFEB in early-stage DIC, we collected whole hearts from EC-Tfeb Tg and WT mice for single-cell RNA sequencing (scRNA-seq) at 2 weeks, with or without DOX treatment, before the onset of cardiac dysfunction (Figure 6A). Barcode rank plots and quality control metrics were generated to assess the quality of scRNA-seq libraries (Figures S16 through S19). Twenty cell subpopulations were identified in mouse heart tissues (Figure 6B; Figure S20A). Based on specific endothelial markers, ECs were classified into arterial (*Gja5*,<sup>25</sup> *Sema3g*,<sup>26</sup> and *Sox17*<sup>27</sup>), venous (*Nr2f2*,<sup>25,28,29</sup> *Vcam1*,<sup>30</sup> and *Cdh11*<sup>31</sup>), capillary (*Car4*,<sup>30</sup> *Rgcc*,<sup>30</sup> and *Sgk1*<sup>32</sup>), and lymphatic (*Prox1*, *Lyve1*, and *Reln*) EC subtypes. Capillary ECs were further clustered into 2 subpopulations: EC#1 and EC#2. It is interesting that DOX treatment altered the proportions of capillary EC#1 and EC#2, indicating that capillary ECs are susceptible to DOX-induced toxicity at an early stage. TFEB transgene reversed the effect of DOX on capillary ECs (Figure 6C). Pathway analysis using single-cell pathway analysis revealed that, compared with capillary EC#1, capillary EC#2 exhibits more pronounced pathway activity related to TNFA\_SIGNALING\_VIA\_NFKB and INFLAMMATORY\_RESPONSE (Figure S20B). Furthermore, differential gene expression analysis of scRNA-seq data showed that the expression frequencies of *Tfeb* and *Dab2* were reduced in cardiac ECs treated with DOX (Figure 6D). Pathway analysis indicated that multiple signaling pathways, including REGULATION\_OF\_AUTOPHAGY, APICAL\_JUNCTION, ENDOCYTOSIS, and LYSOSOME\_VESICLE\_BIOGENESIS, were enriched in EC-Tfeb Tg mice, whereas APOPTOSIS, TNFA\_SIGNALING\_VIA\_NFKB, and IL6\_JAK\_STAT3\_SIGNALING pathways were enriched in WT mice under DOX treatment (Figure 6E). Collectively, the multiple critical pathways identified through scRNA-seq analysis are consistent with those revealed by in vitro RNA sequencing data, providing mechanistic insight into the protective effects of TFEB on EC function.

## Endothelial TFEB Preserves EC-Cardiomyocyte Communication, Attenuates EC Barrier Damage, and Improves Cardiomyocyte Contractile Function Under DOX Treatment

ECs interact with cardiomyocytes and affect cardiomyocyte function.<sup>33</sup> The intercellular communication

**Figure 5. TFEB inhibits proinflammatory cytokine release by upregulation of DAB2.**

**A**, A Venn diagram was used to integrate 4 different gene lists: upregulated genes in TFEB-overexpressing human umbilical vein ECs (HUVECs) treated with DOX (3370 genes), upregulated genes in TFEB-overexpressing HUVECs treated with vehicle (3267 genes), TFEB target genes from a chromatin immunoprecipitation sequencing (ChIP-seq) data set in HUVECs (GSE88894, 1002 genes), and genes in the autophagosome-lysosomal pathway (ALP; 891 genes). **B**, Reanalysis of ChIP-seq data set (GSE88894) identified potential TFEB binding sites in the (Continued)

**Figure 5 Continued.** promoter region of human DAB2. **C**, HUVECs were infected with adenovirus encoding LacZ (AdLacZ) or Flag-TFEB (AdFlag-TFEB, 20 multiplicity of infection [MOI]). Twenty-four hours later, chromatin immunoprecipitation with quantitative polymerase chain reaction (ChIP-qPCR) was performed to measure TFEB enrichment at the DAB2 promoter (3 individual primer pairs) and normalized to 10% input. IgG was used as a negative control ( $n=5$ ). **D**, A luciferase reporter assay was performed by cotransfected HEK293FT cells with control (DAB2 nonpromoter region), DAB2-promoter, and DAB2-promoter with deletion of TFEB binding region (illustrated). Firefly and Renilla luciferase activities were measured by a luminometer ( $n=5$ ). **E**, HCMECs were transfected with siCtrl or siTFEB (20 nM) for 48 hours and then treated with DOX (1  $\mu$ M) for 24 hours. DAB2 expression was measured by Western blot ( $n=5$ ). **F**, The expression of DAB2 in MCMECs from wild-type (WT) and EC-*Tfeb* Tg mice was measured by Western blot and quantified ( $n=6$ ). **G**, HUVECs stably overexpressing TFEB and control ECs were treated with DOX (1  $\mu$ M). At the indicated time points, DAB2 expression was assessed by Western blot and quantified ( $n=6$ ). **H**, HCMECs were transfected with siCtrl or siDAB2 (20 nM) for 48 hours, followed by incubation with MitoSOX (5  $\mu$ M) for 30 min. ROS production was determined by flow cytometry ( $n=5-9$ ). **I**, HUVECs stably expressing mCherry-EGFP-LC3 (C-G-LC3-EC) were transfected with siCtrl or siDAB2 (20 nM) for 48 hours and then treated with DOX (1  $\mu$ M) for 24 hours. Autophagic flux was assessed by flow cytometry ( $n=6$ ). **J** and **K**, HUVECs stably overexpressing TFEB and control ECs were treated with DOX (1  $\mu$ M) for 24 hours. The release of IL-6 (**J**) and IL-1 $\beta$  (**K**) into the culture medium was determined by ELISA ( $n=5$  in **J** and  $n=5$  or 6 in **K**). Data in **C**, **D**, and **F** were analyzed by an unpaired *t* test. Data in **E** were analyzed by 2-way ANOVA. Data in **G** through **K** were analyzed by 2-way ANOVA followed by Tukey post hoc test. Data are presented as mean  $\pm$  SEM; \* $P<0.05$ , \*\* $P<0.01$ , \*\*\* $P<0.001$ .

was analyzed using the integrated scRNA-seq data based on ligand-receptor interactions. The chord diagram indicated that DOX significantly altered the pattern of EC-cardiomyocyte communications, but EC TFEB transgene preserved these interactions under DOX treatment (Figure 7A). Specifically, DOX reduced both the number and strength of EC-cardiomyocyte interactions in WT mice, whereas EC-*Tfeb* Tg enhanced interaction strength under DOX treatment conditions (Figure S21A). We also identified signaling ligand-receptor pairs between ECs and cardiomyocytes that were significantly regulated by DOX and EC-*Tfeb* Tg under vehicle control or DOX treatment conditions (Figure S21B through S21D). Endothelium acts as the primary barrier against excessive uptake of DOX in tissues. In vitro, we conducted a transendothelial permeability assay using fluorescein isothiocyanate (FITC)-dextran, which was added to the upper chamber. After DOX treatment, we observed an average 40.6% increase in the FITC fluorescence intensity ratio (bottom chamber versus upper chamber) in the medium from control ECs and an average 14.6% increase in medium from TFEB-overexpressing ECs (Figure 7B). Similarly, EC TFEB transgene significantly reduced DOX-induced FITC-dextran leakage (Figure 7C). Therefore, EC TFEB could attenuate the exposure of cardiomyocytes to excessive DOX by reducing EC barrier permeability. CLDN11 (claudin-11), a marker of cardiac valvular ECs<sup>34</sup> and a member of the claudin family, plays a crucial role in forming cell-cell tight junctions, regulating paracellular permeability, and maintaining EC barrier function. We found that TFEB upregulated CLDN11 in ECs, both in the presence and absence of DOX, whereas DAB2 deficiency exacerbated DOX-induced downregulation of CLDN11 and attenuated the TFEB-dependent upregulation of CLDN11 (Figure 7D). In vitro coculture of ECs and human induced pluripotent stem cells–cardiomyocytes was used to investigate the effects of EC TFEB on cardiomyocyte function, including contractility and calcium flux. EC TFEB protected cardiomyocytes against DOX-

induced slowing of contractile kinetics and impaired calcium handling (Figure 7E). Together, these findings indicate that TFEB protects cardiomyocyte function by preserving EC barrier integrity and EC-cardiomyocyte communication.

## EC TFEB Increases Myocardial Viability and EC-Specific *Dab2* Knockdown Abolishes Its Protective Effect on Cardiac Dysfunction in Tumor-Bearing Mice Treated With DOX

DOX is widely used to treat various cancers, including sarcoma. Of clinical relevance, the expression levels of TFEB and DAB2 are positively correlated with overall survival in patients with sarcoma (Figure S22). DAB2 is upregulated in ECs treated with tumor-conditioned medium, highlighting its relevance in cancer-related conditions (Figure S23A). To investigate the protective role of EC TFEB in the context of tumor burden, we generated a fibrosarcoma model using MCA205 cells in WT and EC-*Tfeb* Tg mice treated with DOX. <sup>18</sup>F-fluorodeoxyglucose positron emission tomography/computed tomography enables a noninvasive viability assessment of the heart and tumor simultaneously after chemotherapy. The standardized uptake value normalized to body weight was used as a semi-quantitative measurement of radiotracer uptake. Compared with WT mice, EC-*Tfeb* Tg mice showed higher uptake of <sup>18</sup>F-fluorodeoxyglucose in heart tissue but no significant changes in tumor uptake (Figure 8A). The permeability of mouse cardiac and tumor vessels was evaluated using FITC-dextran perfusion. EC-*Tfeb* Tg reduced vascular leakage in heart tissue, indicated by decreased FITC-dextran accumulation outside damaged vasculature, but it had no significant effect on vascular leakage in tumors (Figure 8B and 8C). To test whether DAB2 is essential for the protective effect of EC TFEB on cardiac function, we silenced endothelial *Dab2* in EC-*Tfeb* Tg mice using AAV2-QuadYF-sh*Dab2*, which specifically targets ECs in vivo. The

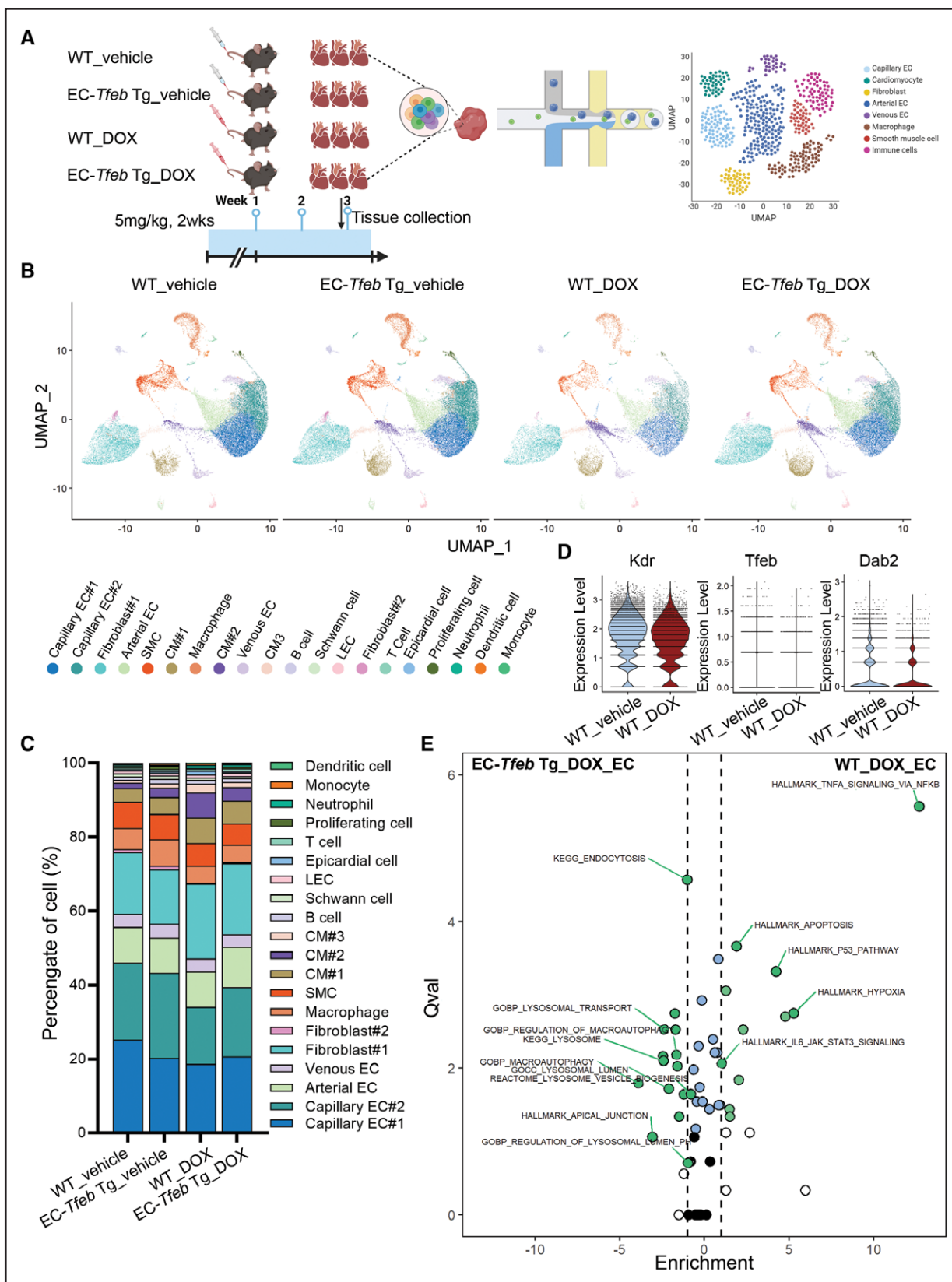


**Figure 6. Single-cell RNA sequencing (scRNA-seq) analysis indicates that EC TFEB enhances autophagy, lysosomal function, and endocytosis in MCMECs in EC-*Tfeb* Tg mice treated with DOX.**

**A**, Flowchart of scRNA-seq analysis of mouse heart tissues from male EC-*Tfeb* Tg mice and wild-type (WT) mice treated with DOX (5 mg/kg IV once a week) or vehicle for 2 weeks (n=4 or 5 per group). Single cells were isolated from mice and subjected to scRNA-seq analysis. **B**, Twenty cell clusters were identified after PCA. **C**, Proportions of the cell clusters detected by scRNA-seq. Cell types were assigned using (Continued)

**Figure 6 Continued.** both automatic annotation software scCATCH (v3.2.2) and manual curation. **D**, Differential expression of *Kdr*, *Tfeb*, and *Dab2* in ECs was analyzed using MAST and visualized with volcano plot. **E**, The Single Cell Pathway Analysis (SCPA) package was used to compare pathway analysis in scRNA-seq data to compare EC subpopulations in EC-*Tfeb* Tg and WT mice treated with DOX. Q-value (Qval) was used as the primary statistic for evaluating biological relevance, with pathway fold change serving as a secondary informative metric. A larger Qval reflects a greater change in pathway “activity.”

efficiency of *Dab2* knockdown in ECs was confirmed (Figure S23B). Cardiac function in tumor-bearing mice was assessed before and after DOX treatment. Loss of *Dab2* exacerbated DOX-induced cardiac dysfunction and abolished the protective effect in EC-*Tfeb* Tg mice (Figure 8D). DOX treatment significantly inhibited tumor growth in both WT and EC-*Tfeb* Tg mice compared with untreated controls, with no significant difference in tumor growth observed between WT and EC-*Tfeb* Tg mice after DOX treatment (Figure 8E). The specificity of AAV2-QuadYF targeting ECs was validated by GFP and ICAM-2 double immunostaining in mouse heart tissues (Figure 8F). *Dab2* knockdown in ECs abolished the TFEB-dependent preservation of cardiac vascular density under DOX treatment (Figure 8G). Collectively, these results demonstrate that EC TFEB enhances heart viability and DAB2 mediates the protective effects of EC TFEB on cardiac function in the setting of tumor burden and DOX treatment. To rule out the influence of tumor-derived stress, we assessed cardiac function in non-tumor-bearing mice with EC-*Dab2* silencing or WT controls. EC-*Dab2* silencing significantly impaired cardiac function, elevated IL-6 and IL-1 $\beta$  levels in heart tissue, and increased perivascular fibrosis in those non-tumor-bearing mice (Figure S24). These findings underscore the critical protective role of endothelial *Dab2* against cardiac dysfunction, regardless of tumor presence.

## DISCUSSION

This study investigated the role of EC TFEB in DIC using a chronic cardiac toxicity mouse model. Our data suggest that EC TFEB increases mouse survival, improves cardiac function, and inhibits perivascular fibrosis in vivo. TFEB exhibited antiapoptotic, antioxidant stress, autophagy/lysosomal modulation, and anti-inflammatory effects in ECs treated with DOX. Mechanistically, DAB2 was identified as a TFEB target gene and mediated the protective effects of TFEB on EC damage and cardiac dysfunction under DOX treatment.

EC dysfunction is recognized to play a critical role in the onset and severity of cardiotoxicity associated with chemotherapy.<sup>35</sup> Because the initial EC insult is likely asymptomatic, there is often a long delay between the termination of chemotherapy and the onset of cardiovascular disorders.<sup>36</sup> This calls on detailed investigations elaborating the mechanisms underlying cancer therapy-induced EC dysfunction and cardiotoxicity.

Our findings suggest that TFEB responds to chemotherapeutic drugs and preserves EC function to maintain vascular homeostasis and cardiac function. DOX impairs cardiac function, particularly left ventricular function, which may contribute to pulmonary congestion. We acknowledge that DOX may also directly damage lung tissue. In addition, we cannot rule out a direct protective effect of EC TFEB on lung vasculature under DOX treatment conditions. The detailed mechanisms underlying pulmonary congestion warrant further investigation. The mild hepatic congestion observed may be a result of the treatment regimen and the timing of the observation end point, highlighting tissue-specific differences in congestion severity after DOX treatment.

Elevated production of ROS can cause progressive damage to mitochondrial DNA, ultimately resulting in apoptosis-mediated loss of ECs. Our data demonstrated that TFEB promotes EC survival and reduces ROS production in the presence of DOX. Autophagy maintains cell and tissue homeostasis, especially during stress, by forming autophagosomes that fuse with lysosomes for cargo degradation.<sup>37</sup> DOX can disrupt lysosome function through several mechanisms, including lysosome membrane permeabilization, inhibition of lysosome enzymes, disruption of lysosomal acidification, and inhibition of autophagosome-lysosome fusion.<sup>38</sup> Long-term DOX treatment inhibits autophagy and lysosomal function. In this study, we observed increased autophagic flux but impaired autolysosomes in ECs within 24 hours of DOX treatment, indicating that the short-term treatment with DOX at clinically used dosage cannot hamper autophagic flux in ECs. Indeed, TFEB positively regulates autophagy and plays a critical role in autophagosome processing and lysosomal function. In ECs, TFEB can increase lysosomal biogenesis, thereby preventing severe autophagosome accumulation caused by DOX-induced lysosome dysfunction. Altogether, multiple mechanisms, including inhibition of ROS and apoptosis and activation of the autophagy-lysosomal pathway, contribute to the protective effects of TFEB in ECs.

As a transcription factor, TFEB regulates numerous genes and signaling pathways beyond the autophagy-lysosomal pathway. In the present study, we focused on the role of TFEB in apoptosis, autophagy, ROS, and inflammation. However, TFEB may also counteract the negative effects of DOX on other signaling pathways. DAB2 is a clathrin- and cargo-binding endocytic adaptor protein that plays a role in endocytosis,<sup>39</sup> cell

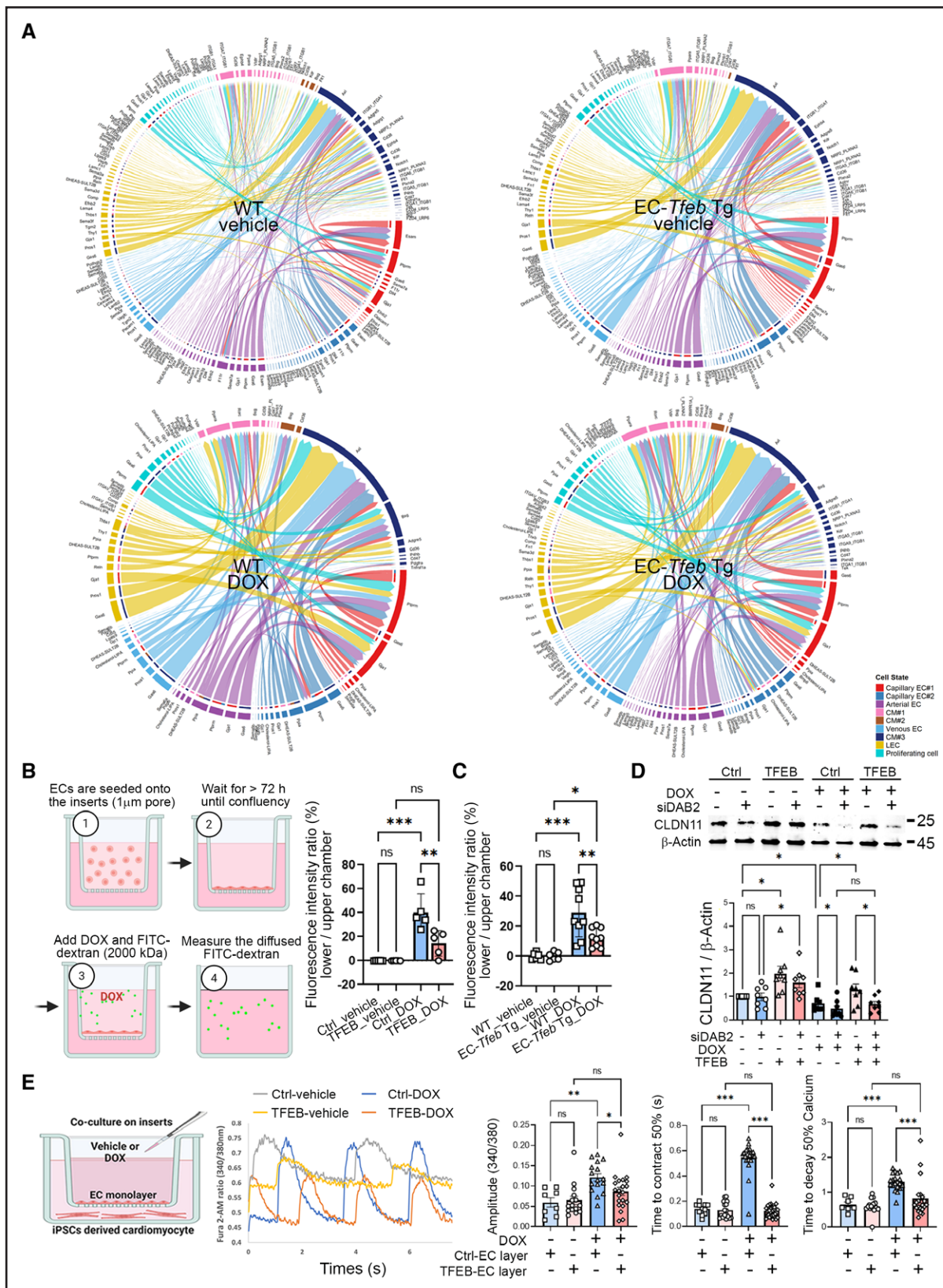


**Figure 7. Endothelial TFEB maintains EC-cardiomyocyte (CM) communication, ameliorates EC barrier damage, and prevents CM hypercontractility after DOX treatment.**

**A**, EC (source)–CM (target) communication was analyzed by CellChat (v2) using the scRNA-seq data from wild-type (WT) and EC-*Tfeb* Tg mice treated with either vehicle or DOX. A chord diagram was used to visualize cell-cell communication based on ligand-receptor interactions ( $n=4$  or 5 per group). **B**, HUVECs stably overexpressing TFEB and control ECs were cultured on the membrane of transwell inserts and (Continued)

**Figure 7 Continued.** treated with DOX (1  $\mu$ M) for 24 hours. FITC-dextran was used to assess transendothelial cell permeability as illustrated (n=5). **C**, Transendothelial cell permeability was measured in MCMECs from WT and EC-Tfeb Tg mice (n=6–9), as described in **B**. **D**, Expression of CLDN11 was determined by Western blot (n=8). **E**, Schematic of the in vitro coculture model comprising HUVECs stably overexpressing TFEB or control ECs and human induced pluripotent stem cell (iPSC)-derived CMs. ECs (upper chamber) were treated with vehicle (n=8–15) or DOX (1  $\mu$ M, n=16–21) for 24 hours. The effects of EC TFEB on iPSC-derived CM function in the lower chamber, including CM contractility, and calcium flux were determined using IonOptix Calcium Imaging System. Data in **B** and **C** were analyzed by 2-way ANOVA; **E** was analyzed by 1-way ANOVA followed by Tukey post hoc test. Data are presented as mean $\pm$ SEM; \*P<0.05, \*\*P<0.01, \*\*\*P<0.001.

adhesion, and signal transduction. Initially identified as a tumor suppressor,<sup>40</sup> DAB2 negatively regulates critical signaling pathways such as Wnt, MAPK, and TGF- $\beta$ , which are involved in promoting tumor growth. Silencing DAB2 in bone marrow–derived dendritic cells activates PI3K and NF- $\kappa$ B, leading to increased expression of proinflammatory cytokines IL-6 and IL-12.<sup>41</sup> In liver sinusoidal ECs, DAB2 promotes the internalization of VEGFR1 and VEGFR2, which are necessary for angiogenesis-related processes.<sup>42</sup> During early-stage cardiac development, *Dab2* is expressed in the ventral mesoderm and pronephros, and in late stages, it is mainly found in the developing endothelium.<sup>43</sup> It is thought to play a crucial role in lysosome fusion by interacting with RhoA GTPase, which increases the activity of lysosome fusion proteins.<sup>44</sup> Similar to previous findings showing that DAB2 deficiency induces proinflammatory effect in dendritic cells and myeloid cells, our data indicate that DAB2 deletion not only promotes inflammatory response but also increases ROS production and reduces autophagic flux in ECs. However, the role of DAB2 in antagonizing the effects of DOX on EC dysfunction has yet to be determined. Our findings revealed that DAB2 is a TFEB target gene, and DAB2 is essential for TFEB to restrict proinflammatory cytokine release from ECs. Lysosomal exocytosis promotes cellular clearance,<sup>45</sup> and DAB2 may mediate the effect of TFEB on lysosomal exocytosis, warranting future studies.

The elimination half-life of DOX in tissues is 20 to 48 hours in patients. DOX impairs cardiac function through multiple levels of damage: increased vascular permeability, damaged vascular structure (perivascular fibrosis), and cardiomyocyte toxicity. Indeed, ECs and cardiomyocytes communicate through direct cell-cell interactions and paracrine signaling, including growth factors, cytokines, and extracellular vesicles.<sup>46</sup> Our scRNA-seq analysis identified signaling ligand-receptor pairs between ECs and cardiomyocytes that are significantly regulated by DOX and EC-Tfeb Tg under vehicle control or DOX treatment conditions, providing valuable insights into EC-cardiomyocyte communication and warranting follow-up functional studies. Moreover, the data suggest that EC TFEB inhibits the release of proinflammatory cytokines (IL-1 $\beta$  and IL-6) from MCMECs, which could at least partially account for the protective effects of EC TFEB on cardiomyocyte function. The scRNA-seq analysis identified 2 capillary

EC subpopulations with distinct gene signatures and pathway enrichments. These differences likely underlie the observed shift between the 2 populations after DOX treatment and TFEB overexpression, highlighting their distinct functional roles within the capillary endothelium. DOX impairs EC barrier formation, increasing vascular permeability and exacerbating toxicity.<sup>21</sup> EC TFEB significantly reduced DOX-induced EC permeability in vitro and vascular leakage in the heart in vivo. Collectively, attenuated proinflammatory cytokine release from ECs, preserved EC-cardiomyocyte communications, and maintained EC barrier contribute to the protective effects of TFEB on cardiomyocyte function.

TFEB has distinct effects on cardiomyocyte function depending on the pathological conditions. Myocardial TFEB was impaired in cardiac proteinopathy and forced TFEB overexpression protected against proteotoxicity in cardiomyocytes.<sup>47</sup> During glucolipotoxicity, reduced TFEB expression rendered cardiomyocyte susceptible to cardiac injury.<sup>48</sup> DOX decreased cardiomyocyte viability by reducing TFEB expression.<sup>49</sup> A recent study found that cardiomyocyte-specific *Tfeb* knockout attenuated DIC, and TFEB/GDF15 pathway exacerbates DOX cardiotoxicity.<sup>50</sup> TFEB could either protect or contribute to cardiomyocyte death according to the varied pathological conditions. However, our data show that endothelial TFEB prevents EC damage and mitigates cardiac dysfunction in vivo by reducing apoptosis, ROS, fibrosis, and vascular leakage, highlighting its cell type-dependent effects in DIC.

A limitation of this study is the exclusive use of male mice, chosen because of the higher incidence of sarcoma and fibrosarcoma in human males compared with females. Future investigation using female-specific models, such as breast cancer models, is warranted to explore the role of endothelial TFEB in females and to assess potential sex-dependent differences in response.

In conclusion, endothelial TFEB inhibits DIC by protecting against EC toxicity through multiple mechanisms. Our findings provide evidence showing that DAB2 is a TFEB target gene, and it is required for the protective effects of TFEB on EC and cardiac function under DOX treatment. This study demonstrated that EC TFEB is a potential target to preserve vascular and cardiac function during chemotherapy.

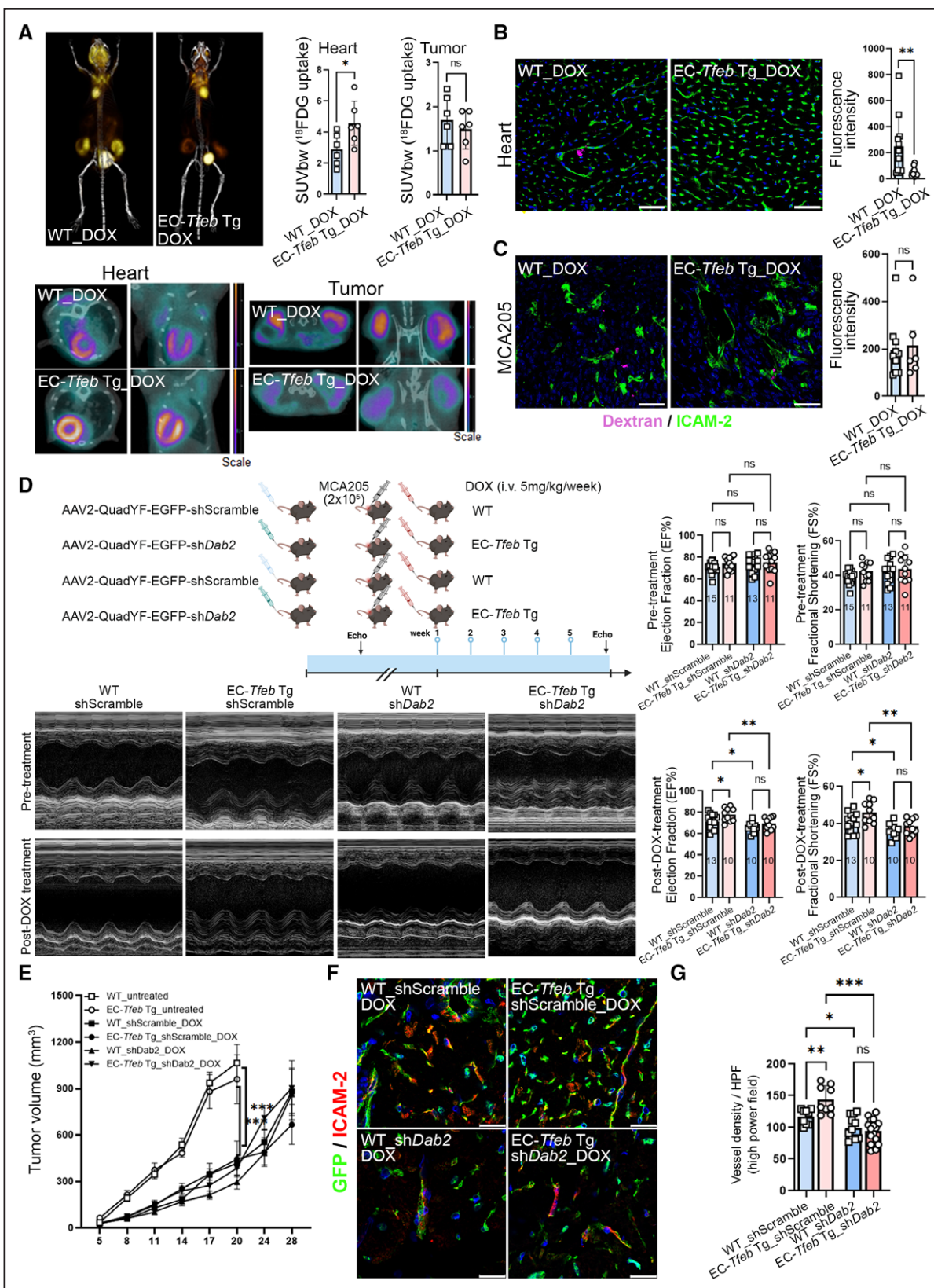


**Figure 8. EC TFEB enhances myocardial viability and DAB2 mediates the protective effects of EC TFEB on DIC in tumor-bearing mice.**

A through C, Fibrosarcoma cells (MCA205, 2×10<sup>5</sup>) were subcutaneously injected into the flanks of male wild-type (WT) and EC-Tfeb Tg mice, followed by DOX treatment (5 mg/kg IV, once a week). **A**, After 4 weeks of DOX treatment, heart tissue viability was evaluated using <sup>18</sup>F-fluorodeoxyglucose (FDG) positron emission tomography (PET)/CT imaging (n=6 per group). **B** and **C**, After 5 weeks of (Continued)

**Figure 8 Continued.** DOX treatment, vascular permeability in mouse hearts (**B**) and tumors (**C**) was assessed by tail vein injection of FITC-dextran (10 kDa). Accumulated FITC-dextran (purple) was observed in DOX-induced collapsed microvessels. FITC-dextran fluorescence intensity per high-power field (HPF) was quantified using ImageJ (n=11 per group for heart; n=6–10 per group for tumor vascular permeability). Scale bar=100 μm. **D** through **G**, EC-specific AAV2-QuadYF expressing either mouse *Dab2* shRNA or scramble shRNA was administered intravenously into male EC-*Tfeb* Tg or WT mice. After 3 weeks, the fibrosarcoma model was established, and mice were treated with DOX (5 mg/kg IV once weekly for 5 weeks). **D**, Ejection fraction and fractional shortening were assessed before and after DOX treatment (n=11–15 per group). **E**, Tumor growth was monitored in each group (n=15 per group). **F**, Immunostaining of ICAM-2 (an EC marker) and GFP (from AAV2-QuadYF) in collected heart tissues. **G**, Cardiac vascular density was quantified per HPF (n=9–16 per group). Scale bar=20 μm. Data in **A** through **C** were analyzed by an unpaired *t* test. Data in **D**, **E**, and **G** were analyzed by 2-way ANOVA followed by Tukey post hoc test. Data are presented as mean±SEM; \*P<0.05, \*\*P<0.01, \*\*\*P<0.001.

## ARTICLE INFORMATION

Received August 8, 2024; accepted November 25, 2025.

### Affiliations

Department of Surgery, Division of Vascular Diseases and Surgery, Davis Lung and Heart Institute, College of Medicine (W.D., G.I.K., Y.F.), Department of Radiation Oncology (C.W.), Wexner Medical Center, Ohio State University, Columbus. Department of Cancer Biology (W.D., M.R., G.I.K., L.T.E., C.W., J.-L.G., Y.F.), Department of Internal Medicine, Division of Cardiovascular Health and Diseases (W.H., R.C.B., S.S.), Department of Pharmacology, Physiology, and Neurobiology (D.D., G.-C.F.), Department of Pathology and Laboratory Medicine (Y.W.), College of Medicine, University of Cincinnati, OH.

### Acknowledgments

W.D. and Y.F. designed the study; W.D., M.R., W.H., D.D., G.K., and L.T. carried out the experiments; W.D. analyzed bulk RNA sequencing and scRNA-seq data; D.D. analyzed contractility data; W.D. and Y.F. interpreted the results and drafted the article; Y.W., C.W., S.S., C.F., J.G., and R.B. reviewed and edited the article critically. Y.F. contributed to the conceptualization, supervision, and project administration, and approved the final version for submission. All authors approved the final version for publication and agreed to be accountable for all aspects of the work, ensuring that questions related to the accuracy or integrity of any part of the work are appropriately investigated and resolved. We extend our appreciation to the Live Microscopy Core, Genomics, Epigenomics, and Sequencing Core, and Advanced Cell Analysis Service Center at the University of Cincinnati for their invaluable support and services. We gratefully acknowledge the staff of the University of Cincinnati Preclinical Imaging Core, especially Lisa Lemen and Xiangning Wang.

### Sources of Funding

This work was supported by the National Institutes of Health (R01HL171495 to Y.F. and W.D.; R01HL145176, 3R01HL145176-02S1, and R01HL167024 to Y.F.; R01 HL130356, R01 HL105826, and R01 HL143490 to S.S.; R01 HL168464 to Y.W. and W.H.; R01 HL157456 to Y.W. and J.L.) and the American Heart Association (Transformation Project Award No. 945748 to S.S.; predoctoral fellowship No. 20PRE35120272 to D.D.).

### Disclosures

Dr Sadayappan provides consulting and collaborative research studies to Red Saree Inc, Alexion, Regen Therapeutics, and Affinia Therapeutics Inc, but such work is unrelated to the content of this article. The other authors report no conflicts.

### Supplemental Material

#### Checklist

#### Expanded Supplemental Methods

#### Figures S1–S24

#### Tables S1–S3

#### References 51–71

## REFERENCES

- Johnson-Arbor K, Dubey R. Doxorubicin. In: *StatPearls*. Treasure Island (FL); 2024.
- Arola OJ, Saraste A, Pulkki K, Kallajoki M, Parvinen M, Voipio-Pulkki LM. Acute doxorubicin cardiotoxicity involves cardiomyocyte apoptosis. *Cancer Res*. 2000;60:1789–1792.
- Pinto AR, Ilinykh A, Ivey MJ, Kuwabara JT, D'Antoni ML, Debuque R, Chandran A, Wang L, Arora K, Rosenthal NA, et al. Revisiting cardiac cellular composition. *Circ Res*. 2016;118:400–409. doi: 10.1161/CIRCRESAHA.115.307778
- Litvinukova M, Talavera-Lopez C, Maatz H, Reichart D, Worth CL, Lindberg EL, Kanda M, Polanski K, Heinig M, Lee M, et al. Cells of the adult human heart. *Nature*. 2020;588:466–472. doi: 10.1038/s41586-020-2797-4
- M Bosman HB, Franssen C, Kruger DN, Neutel CHG, Favere K, Van Asbroeck B, Goovaerts I, De Meyer GRY, Van Craenenbroeck EM, Guns PJDF. Doxorubicin induces measurable vascular toxicity: assessment in a clinical and preclinical study. *Cardiovasc Res*. 2022;118: doi: 10.1093/cvr/cvac066.181
- Todorova VK, Wei JY, Makhlouf I. Subclinical doxorubicin-induced cardio-toxicity update: role of neutrophils and endothelium. *Am J Cancer Res*. 2021;11:4070–4091.
- Wang L, Yu P, Zhou B, Song J, Li Z, Zhang M, Guo G, Wang Y, Chen X, Han L, et al. Single-cell reconstruction of the adult human heart during heart failure and recovery reveals the cellular landscape underlying cardiac function. *Nat Cell Biol*. 2020;22:108–119. doi: 10.1038/s41556-019-0446-7
- Pommier Y, Leo E, Zhang H, Marchand G. DNA topoisomerase and their poisoning by anticancer and antibacterial drugs. *Chem Biol*. 2010;17:421–433. doi: 10.1016/j.chembiol.2010.04.012
- Yarana C, St Clair DK. Chemotherapy-induced tissue injury: an insight into the role of extracellular vesicles-mediated oxidative stress responses. *Antioxidants (Basel)*. 2017;6: doi: 10.3390/antiox6040075
- He H, Wang L, Qiao Y, Zhou Q, Li H, Chen S, Yin D, Huang Q, He M. Doxorubicin induces endotheliotoxicity and mitochondrial dysfunction via ROS/eNOS/NO pathway. *Front Pharmacol*. 2019;10:1531. doi: 10.3389/fphar.2019.01531
- Mameli E, Martello A, Caporali A. Autophagy at the interface of endothelial cell homeostasis and vascular disease. *FEBS J*. 2022;289:2976–2991. doi: 10.1111/febs.15873
- Napolitano G, Ballabio A. TFEB at a glance. *J Cell Sci*. 2016;129:2475–2481. doi: 10.1242/jcs.146365
- Fan Y, Lu H, Liang W, Garcia-Barrio MT, Guo Y, Zhang J, Zhu T, Hao Y, Zhang J, Chen YE. Endothelial TFEB (transcription factor EB) positively regulates postischemic angiogenesis. *Circ Res*. 2018;122:945–957. doi: 10.1161/CIRCRESAHA.118.312672
- Sun J, Lu H, Liang W, Zhao G, Ren L, Hu D, Chang Z, Liu Y, Garcia-Barrio MT, Zhang J, et al. Endothelial TFEB (transcription factor EB) improves glucose tolerance via upregulation of IRS (insulin receptor substrate) 1 and IRS2. *Arterioscler Thromb Vasc Biol*. 2021;41:783–795. doi: 10.1161/ATVBAHA.120.315310
- Zamorano JL, Lancellotti P, Rodriguez Munoz D, Aboyans V, Asteggiano R, Galderisi M, Habib G, Lenihan DJ, Lip GYH, Lyon AR, et al; ESC Scientific Document Group. 2016 ESC position paper on cancer treatments and cardiovascular toxicity developed under the auspices of the ESC Committee for Practice Guidelines: the Task Force for Cancer Treatments and Cardiovascular Toxicity of the European Society of Cardiology (ESC). *Eur Heart J*. 2016;37:2768–2801. doi: 10.1093/eurheartj/ehw211
- Verschoor AJ, Litiere S, Marreaud S, Judson I, Toulmonde M, Wardemann E, LeCesne A, Gelderblom H. Survival of soft tissue sarcoma patients after completing six cycles of first-line anthracycline containing treatment: an EORTC-STBSG database study. *Clin Sarcoma Res*. 2020;10:18. doi: 10.1186/s13569-020-00137-5
- Siegel RL, Miller KD, Jemal A. Cancer statistics, 2020. *CA Cancer J Clin*. 2020;70:7–30. doi: 10.3322/caac.21590
- Cook MB, McGlynn KA, Devesa SS, Freedman ND, Anderson WF. Sex disparities in cancer mortality and survival. *Cancer Epidemiol Biomarkers Prev*. 2011;20:1629–1637. doi: 10.1158/1055-9965.EPI-11-0246
- Buja A, Rugge M, Tropea S, Cozzolino C, Formaro CM, Grotto G, Zorzi M, Vecchiato A, Del Fiore P, Brunello A, et al. Sex differences in soft tissue sarcoma: incidence, clinicopathological profile, survival, and costs. *J Womens Health (Larchmt)*. 2023;32:1257–1264. doi: 10.1089/jwh.2023.0019

20. Tanaka R, Umemura M, Narikawa M, Hikichi M, Osaw K, Fujita T, Yokoyama U, Ishigami T, Tamura K, Ishikawa Y. Reactive fibrosis precedes doxorubicin-induced heart failure through sterile inflammation. *ESC Heart Fail.* 2020;7:588–603. doi: 10.1002/ehf2.12616
21. Wilkinson EL, Sidaway JE, Cross MJ. Cardiotoxic drugs herceptin and doxorubicin inhibit cardiac microvascular endothelial cell barrier formation resulting in increased drug permeability. *Biol Open.* 2016;5:1362–1370. doi: 10.1242/bio.20120362
22. Mauvezin C, Neufeld TP. Bafilomycin A1 disrupts autophagic flux by inhibiting both V-ATPase-dependent acidification and Ca<sup>2+</sup>-P60A/SERCA-dependent autophagosome-lysosome fusion. *Autophagy.* 2015;11: 1437–1438. doi: 10.1080/15548627.2015.1066957
23. Doronzo G, Astanina E, Cora D, Chiabotto G, Comunanza V, Noghera A, Neri F, Puliafito A, Primo L, Spamanato C, et al. TFEB controls vascular development by regulating the proliferation of endothelial cells. *EMBO J.* 2019;38: doi: 10.1525/embj.201798250
24. Di Frusco G, Schulz A, De Cegli R, Savarese M, Mutarelli M, Parenti G, Banfi S, Braultke T, Nigro V, Ballabio A. Lysoplex: an efficient toolkit to detect DNA sequence variations in the autophagy-lysosomal pathway. *Autophagy.* 2015;11:928–938. doi: 10.1080/15548627.2015.1043077
25. Su T, Stanley G, Sinha R, D'Amato G, Das S, Rhee S, Chang AH, Poduri A, Raffrey B, Dinh TT, et al. Single-cell analysis of early progenitor cells that build coronary arteries. *Nature.* 2018;559:356–362. doi: 10.1038/s41586-018-0288-7
26. Vanlandewijck M, He L, Mae MA, Andrae J, Ando K, Del Gaudio F, Nahar K, Lebouvier T, Lavina B, Gouveia L, et al. A molecular atlas of cell types and zonation in the brain vasculature. *Nature.* 2018;554:475–480. doi: 10.1038/nature25739
27. Kim D, Grath A, Lu YW, Chung K, Winkelman M, Schwarz JJ, Dai G. Sox17 mediates adult arterial endothelial cell adaptation to hemodynamics. *Biomaterials.* 2023;293:121946. doi: 10.1016/j.biomaterials.2022.121946
28. dela Paz NG, D'Amore PA. Arterial versus venous endothelial cells. *Cell Tissue Res.* 2009;335:5–16. doi: 10.1007/s00441-008-0706-5
29. You LR, Lin FJ, Lee CT, DeMayo FJ, Tsai MJ, Tsai SY. Suppression of Notch signalling by the COUP-TFII transcription factor regulates vein identity. *Nature.* 2005;435:98–104. doi: 10.1038/nature03511
30. Kalucka J, de Rooij L, Goveia J, Rohlenova K, Dumas SJ, Meta E, Conchinha NV, Taverna F, Teuwen LA, Veys K, et al. Single-cell transcriptome atlas of murine endothelial cells. *Cell.* 2020;180:764–779 e720. doi: 10.1016/j.cell.2020.01.015
31. Schupp JC, Adams TS, Cosme C Jr, Raredon MSB, Yuan Y, Omote N, Poli S, Chioccioli M, Rose KA, Manning EP, et al. Integrated single-cell atlas of endothelial cells of the human lung. *Circulation.* 2021;144:286–302. doi: 10.1161/CIRCULATIONAHA.120.052318
32. Fleming RE, Crouch EC, Ruzicka CA, Sly WS. Pulmonary carbonic anhydrase IV: developmental regulation and cell-specific expression in the capillary endothelium. *Am J Physiol.* 1993;265:L627–L635. doi: 10.1152/ajplung.1993.265.6.L627
33. Hsieh PC, Davis ME, Lisowski LK, Lee RT. Endothelial-cardiomyocyte interactions in cardiac development and repair. *Annu Rev Physiol.* 2006;68:51–66. doi: 10.1146/annurev.physiol.68.040104.124629
34. Feulner L, Wünnemann F, Liang J, Hofmann P, Hitz M-P, Schapiro D, Leclerc S, van Vliet PP, Andelfinger G. Transcriptional dynamics of the murine heart during perinatal development at single-cell resolution. *bioRxiv.* 2024;2024.2003.2005.583423. doi: 10.1101/2024.03.05.583423
35. Luu AZ, Chowdhury B, Al-Omrani M, Teoh H, Hess DA, Verma S. Role of endothelium in doxorubicin-induced cardiomyopathy. *JACC Basic Transl Sci.* 2018;3:861–870. doi: 10.1016/j.jactbs.2018.06.005
36. Grakova EV, Shilov SN, Kopeva KV, Berezikova EN, Popova AA, Neupokoeva MN, Ratushnyak ET, Teplyakov AT. Anthracycline-induced cardiotoxicity: the role of endothelial dysfunction. *Cardiology.* 2021;146:315–323. doi: 10.1159/000512771
37. Terman A, Brunk UT. Autophagy in cardiac myocyte homeostasis, aging, and pathology. *Cardiovasc Res.* 2005;68:355–365. doi: 10.1016/j.cardiores.2005.08.014
38. Li DL, Wang ZV, Ding G, Tan W, Luo X, Criollo A, Xie M, Jiang N, May H, Kyrychenko V, et al. Doxorubicin blocks cardiomyocyte autophagic flux by inhibiting lysosome acidification. *Circulation.* 2016;133:1668–1687. doi: 10.1161/CIRCULATIONAHA.115.017443
39. Morris SM, Arden SD, Roberts RC, Kendrick-Jones J, Cooper JA, Luzio JP, Buss F. Myosin VI binds to and localises with Dab2, potentially linking receptor-mediated endocytosis and the actin cytoskeleton. *Traffic.* 2002;3:331–341. doi: 10.1034/j.1600-0854.2002.30503.x
40. Sheng Z, Sun W, Smith E, Cohen C, Sheng Z, Xu XX. Restoration of positioning control following Disabled-2 expression in ovarian and breast tumor cells. *Oncogene.* 2000;19:4847–4854. doi: 10.1038/sj.onc.1203853
41. Ahmed MS, Byeon SE, Jeong Y, Miah MA, Salahuddin M, Lee Y, Park SS, Bae YS. Dab2, a negative regulator of DC immunogenicity, is an attractive molecular target for DC-based immunotherapy. *Oncoimmunology.* 2015;4:e984550. doi: 10.4161/2162402X.2014.984550
42. Jing Z, Jia-Jun W, Wei-Jie Y. Phosphorylation of Dab2 is involved in inhibited VEGF-VEGFR-2 signaling induced by downregulation of syndecan-1 in glomerular endothelial cell. *Cell Biol Int.* 2020;44:894–904. doi: 10.1002/cbin.11288
43. Kim JD, Kang H, Larrivee B, Lee MY, Mettlen M, Schmid SL, Roman BL, Qyang Y, Eichmann A, Jin SW. Context-dependent proangiogenic function of bone morphogenetic protein signaling is mediated by disabled homolog 2. *Dev Cell.* 2012;23:441–448. doi: 10.1016/j.devcel.2012.07.007
44. Belaid A, Ndiaye PD, Cerezo M, Cailleteau L, Brest P, Klionsky DJ, Carle GF, Hofman P, Mograbi B. Autophagy and SQSTM1 on the RHOA(d) again: emerging roles of autophagy in the degradation of signaling proteins. *Autophagy.* 2014;10:201–208. doi: 10.4161/auto.27198
45. Medina DL, Fraldi A, Bouche V, Annunziata F, Mansuetto G, Spamanato C, Puri C, Pignata A, Martina JA, Sardiello M, et al. Transcriptional activation of lysosomal exocytosis promotes cellular clearance. *Dev Cell.* 2011;21:421–430. doi: 10.1016/j.devcel.2011.07.016
46. Talman V, Kivela R. Cardiomyocyte-endothelial cell interactions in cardiac remodeling and regeneration. *Front Cardiovasc Med.* 2018;5:101. doi: 10.3389/fcvm.2018.00101
47. Pan B, Zhang H, Cui T, Wang X. TFEB activation protects against cardiac proteotoxicity via increasing autophagic flux. *J Mol Cell Cardiol.* 2017;113:51–62. doi: 10.1016/j.yjmcc.2017.10.003
48. Trivedi PC, Bartlett JJ, Perez LJ, Brunt KR, Legare JF, Hassan A, Kienesberger PC, Puliniukunnil T. Glucolipotoxicity diminishes cardiomyocyte TFEB and inhibits lysosomal autophagy during obesity and diabetes. *Biochim Biophys Acta.* 2016;1861:1893–1910. doi: 10.1016/j.bbapap.2016.09.004
49. Bartlett JJ, Trivedi PC, Yeung P, Kienesberger PC, Puliniukunnil T. Doxorubicin impairs cardiomyocyte viability by suppressing transcription factor EB expression and disrupting autophagy. *Biochem J.* 2016;473:3769–3789. doi: 10.1042/BCJ20160385
50. Ozcan M, Guo Z, Valenzuela Ripoll C, Diab A, Picataggi A, Rawnsley D, Loftinaghsh A, Bergom C, Szymanski J, Hwang D, et al. Sustained alternate-day fasting potentiates doxorubicin cardiotoxicity. *Cell Metab.* 2023; doi: 10.1016/j.cmet.2023.02.006
51. Alva JA, Zovein AC, Monvoisin A, Murphy T, Salazar A, Harvey NL, Carmeliet P, Iruela-Arispe ML. VE-cadherin-Cre-recombinase transgenic mouse: a tool for lineage analysis and gene deletion in endothelial cells. *Dev Dyn.* 2006;235:759–767. doi: 10.1002/dvdy.20643
52. Ruifrok AC, Johnston DA. Quantification of histochemical staining by color deconvolution. *Anal Quant Cytol Histol.* 2001;23:291–299.
53. Stewart SA, Palliser D, Mizuno H, Yu EY, Sung An D, Sabatini DM, Chen ISY, Hahn WC, Sharp PA, Weinberg RA, et al. Lentivirus-delivered stable gene silencing by RNAi in primary cells. *RNA.* 2003;9:493–501. doi: 10.1261/rna.2192803
54. Stewart SA, Dykxhoorn DM, Palliser D, Mizuno H, Yu EY, An DS, Sabatini DM, Chen IS, Hahn WC, Sharp PA, et al. Lentivirus-delivered stable gene silencing by RNAi in primary cells. *RNA.* 2003;9:493–501. doi: 10.1261/rna.2192803
55. Ishii S, Matsuura A, Itakura E. Identification of a factor controlling lysosomal homeostasis using a novel lysosomal trafficking probe. *Sci Rep.* 2019;9:11635. doi: 10.1038/s41598-019-48131-2
56. Finak G, McDavid A, Yajima M, Deng J, Gersuk V, Shalek AK, Slichter CK, Miller HW, McElrath MJ, Prlic M, et al. MAST: a flexible statistical framework for assessing transcriptional changes and characterizing heterogeneity in single-cell RNA sequencing data. *Genome Biol.* 2015;16:278. doi: 10.1186/s13059-015-0844-5
57. Subramanian A, Tamayo P, Mootha VK, Mukherjee S, Ebert BL, Gillette MA, Paulovich A, Pomeroy SL, Golub TR, Lander ES, et al. Gene set enrichment analysis: a knowledge-based approach for interpreting genome-wide expression profiles. *Proc Natl Acad Sci U S A.* 2005;102:15545–15550. doi: 10.1073/pnas.0506580102
58. Reimand J, Isolerin R, Voisin V, Kucera M, Tannus-Lopes C, Rostamianfar A, Wadi L, Meyer M, Wong J, Xu C, et al. Pathway enrichment analysis and visualization of omics data using g:Profiler, GSEA, Cytoscape and Enrichment-Map. *Nat Protoc.* 2019;14:482–517. doi: 10.1038/s41596-018-0103-9
59. Gu Z, Eils R, Schlesner M. Complex heatmaps reveal patterns and correlations in multidimensional genomic data. *Bioinformatics.* 2016;32:2847–2849. doi: 10.1093/bioinformatics/btw313

60. N'Diaye EN, Kajihara KK, Hsieh I, Morisaki H, Debnath J, Brown EJ. PLIC proteins or ubiquilins regulate autophagy-dependent cell survival during nutrient starvation. *EMBO Rep.* 2009;10:173–179. doi: 10.1038/embor.2008.238
61. Gump JM, Thorburn A. Sorting cells for basal and induced autophagic flux by quantitative ratiometric flow cytometry. *Autophagy.* 2014;10:1327–1334. doi: 10.4161/auto.29394
62. D'Amato G, Luxan G, de la Pompa JL. Notch signalling in ventricular chamber development and cardiomyopathy. *FEBS J.* 2016;283:4223–4237. doi: 10.1111/febs.13773
63. Li RG, Xu YJ, Ye WG, Li YJ, Chen H, Qiu XB, Yang YQ, Bai D. Connexin45 (GJC1) loss-of-function mutation contributes to familial atrial fibrillation and conduction disease. *Heart Rhythm.* 2021;18:684–693. doi: 10.1016/j.hrthm.2020.12.033
64. Rodriguez-Sinovas A, Sanchez JA, Valls-Lacalle L, Consegal M, Ferreira-Gonzalez I. Connexins in the heart: regulation, function and involvement in cardiac disease. *Int J Mol Sci.* 2021;22. doi: 10.3390/ijms22094413
65. Lu C, Song Y, Wu X, Lei W, Chen J, Zhang X, Liu Q, Deng C, Liang Z, Chen Y, et al. Pleiotropic role of GAS6 in cardioprotection against ischemia-reperfusion injury. *J Adv Res.* 2025;70:481–497. doi: 10.1016/j.jare.2024.04.020
66. Page JH, Ma J, Rexrode KM, Rifai N, Manson JE, Hankinson SE. Plasma dehydroepiandrosterone and risk of myocardial infarction in women. *Clin Chem.* 2008;54:1190–1196. doi: 10.1373/clinchem.2007.099291
67. Thijs L, Fagard R, Forette F, Nawrot T, Staessen JA. Are low dehydroepiandrosterone sulphate levels predictive for cardiovascular diseases? A review of prospective and retrospective studies. *Acta Cardiol.* 2003;58:403–410. doi: 10.2143/AC.58.5.2005304
68. Shufelt C, Bretsky P, Almeida CM, Johnson BD, Shaw LJ, Azziz R, Braunstein GD, Pepine CJ, Bittner V, Vido DA, et al. DHEA-S levels and cardiovascular disease mortality in postmenopausal women: results from the National Institutes of Health–National Heart, Lung, and Blood Institute (NHLBI)-sponsored Women's Ischemia Syndrome Evaluation (WISE). *J Clin Endocrinol Metab.* 2010;95:4985–4992. doi: 10.1210/jc.2010-0143
69. Wu X, Sagave J, Rutkovskiy A, Haugen F, Baysa A, Nygard S, Czibik G, Dahl CP, Gullesstad L, Vaage J, et al. Expression of bone morphogenetic protein 4 and its receptors in the remodeling heart. *Life Sci.* 2014;97:145–154. doi: 10.1016/j.lfs.2013.12.030
70. Lu G, Ge Z, Chen X, Ma Y, Yuan A, Xie Y, Pu J. BMP6 knockdown enhances cardiac fibrosis in a mouse myocardial infarction model by up-regulating AP-1/CEMIP expression. *Clin Transl Med.* 2023;13:e1296. doi: 10.1002/ctm.21296
71. Tang Z, Kang B, Li C, Chen T, Zhang Z. GEPIA2: an enhanced web server for large-scale expression profiling and interactive analysis. *Nucleic Acids Res.* 2019;47:W556–W560. doi: 10.1093/nar/gkz430



# Circulation

## FIRST PROOF ONLY